İSTANBUL TECHNICAL UNIVERSITY ★ INSTITUTE OF SCIENCE AND TECHNOLOGY

POLYMER/CLAY NANOCOMPOSITES FROM SUGAR INDUSTRY BY-PRODUCT

M.Sc. Thesis by
Nurhan KADAK

Department : Polymer Science and Technology

Programme : Polymer Science and Technology

Thesis Supervisor: Prof. Dr. Oya G. ATICI

JUNE 2009

İSTANBUL TECHNICAL UNIVERSITY ★ INSTITUTE OF SCIENCE AND TECHNOLOGY

POLYMER/CLAY NANOCOMPOSITES FROM SUGAR INDUSTRY BY-PRODUCT

M.Sc. Thesis by
Nurhan KADAK
(515071016)

Date of submission : 04 May 2009
Date of defence examination: 03 June 2009

Supervisor (Chairman) : Prof. Dr. Oya G. ATICI (ITU)
Members of the Examining Committee : Prof. Dr. Ahmet AKAR (ITU)
Prof. Dr. A. Tunçer ERCİYES (ITU)

JUNE 2009

İSTANBUL TEKNİK ÜNİVERSİTESİ ★ FEN BİLİMLERİ ENSTİTÜSÜ

ŞEKER PANCARI YAN ÜRÜNÜNDEN POLİMER/KİL NANOKOMPOZİT ELDESİ

YÜKSEK LİSANS TEZİ
Nurhan KADAK
(515071016)

Tezin Enstitüye Verildiği Tarih : 04 Mayıs 2009
Tezin Savunulduğu Tarih : 03 Haziran 2009

Tez Danışmanı : Prof. Dr. Oya G. ATICI (İTÜ)
Diğer Jüri Üyeleri : Prof. Dr. Ahmet AKAR (İTÜ)
Prof. Dr. A. Tunçer ERCİYES (İTÜ)

HAZİRAN 2009

FOREWORD

This study was carried out in Istanbul Technical University, Institute of Science and Technology, Polymer Science and Technology Department.

I would like to express my gratitude to my supervisor Prof. Dr. Oya G. ATICI who shared her knowledge and experience generously, for her encouragement and supports.

I would like to thank Teaching Asistant H. Cüneyt Ünlü, for his help and patience throughout laboratory studies, and all of my colleagues.

I am also grateful to my family for their support and understanding.

June 2009

Nurhan KADAK
Chemist

TABLE OF CONTENTS

Page

ABBREVIATIONS

SAN	**:** Poly(styrene-*co*-acrylonitrile)
PCN	**:** Polymer-Clay Nanocomposite
Mt	**:** Montmorillonite
NaMt	**:** Na-Montmorillonite
MSAN	**:** Molasses-mediated poly(styrene-*co*-acrylonitrile)
MSAN/NaMt	**:** Molasses-mediated poly(styrene-*co*-acrylonitrile)-NaMt nanocomposite
FT-IR	**:** Fourier Transform Infrared Spectroscopy
^{1}H-NMR	**:** Proton Nuclear Magnetic Resonance Spectroscopy
XRD	**:** X-Ray Diffraction
DSC	**:** Differential Scanning Calorimetry
TGA	**:** Thermal Gravimetric Analysis
DMA	**:** Dynamic Mechanical Analysis
TEM	**:** Transmission Electron Microscopy
SEM	**:** Scanning Electron Microscopy
MC	**:** Methyl Cellulose
MHPC	**:** Methyl Hydroxy Propyl Cellulose
AIBN	**:** 2,2'-Azodiisobutyronitrile or Azobisisobutyronitrile
KPS	**:** Potassium Persulfate
DTAB	**:** Dodecyltrimethylammonium Bromide
SDBS	**:** Sodium Dodecylbenzenesulfonate
ABS	**:** Acrylonitrile Butadiene Styrene Rubber
DMF	**:** Dimethylformamide
MSG	**:** Monosodium Glutamate

LIST OF TABLES

Page

LIST OF FIGURES

Page

POLYMER/CLAY NANOCOMPOSITES FROM SUGAR INDUSTRY BY-PRODUCT

SUMMARY

Sugar beet molasses is primarily a by-product of sugar production. Beside water, reducing monosaccharides (raffinose, glucose, fructose and unseperated sucrose etc.), and the materials except monosaccharides constitute the composition of molasses. The sugar content accepted for sugar beet molasses is 46-48%. Molasses is used in a number of industries generally as a major component in compound feeds, livestock feeds and silage additives.

Poly(styrene-*co*-acrylonitrile) (SAN) is the copolymer of styrene and acrylonitrile monomers. Due to their rigidity, transparency, and thermal stability, SAN resins have found applications for dials, knobs, and covers for domestic appliances, electrical equipment, car equipment, dishwasher safe housewares, such as refrigerator meat and vegetable drawers, blender bowls, vacuum cleaner parts, humidifier parts, plus other industrial and domestic applications with requirements more stringent than can be met by polystyrene. SAN resins are also reinforced with glass to make dashboard components and battery cases.

In this study; molasses, containing monosaccharides such as glucose, fructose, raffinose, unseperated sucrose etc., was utilized in the polymerization of styrene and acrylonitrile. Monosaccharides are the molecules which include alcohol groups. Monosaccharide molecule and Ce(IV) produce a complex and decompose to generate free radical (1). Molasses acted as reducing agent to reduce Ce(IV) to Ce(III).

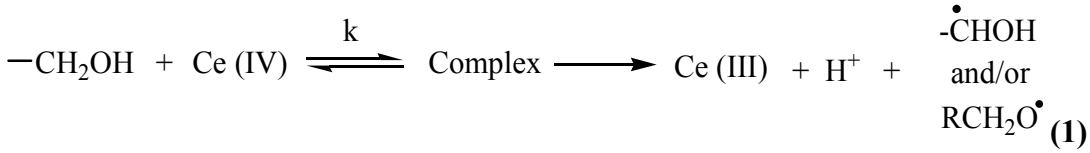

(1)

In this way, free radicals were generated on monosaccharides to initiate polymerization (2). Monosaccharide-mediated poly(styrene-*co*-acrylonitrile) (MSAN) was synthesized by emulsion polymerization. Experiments were performed to obtain optimum reaction conditions (MSAN78). Optimum reaction condition was performed to synthesize polymer-clay nanocomposites.

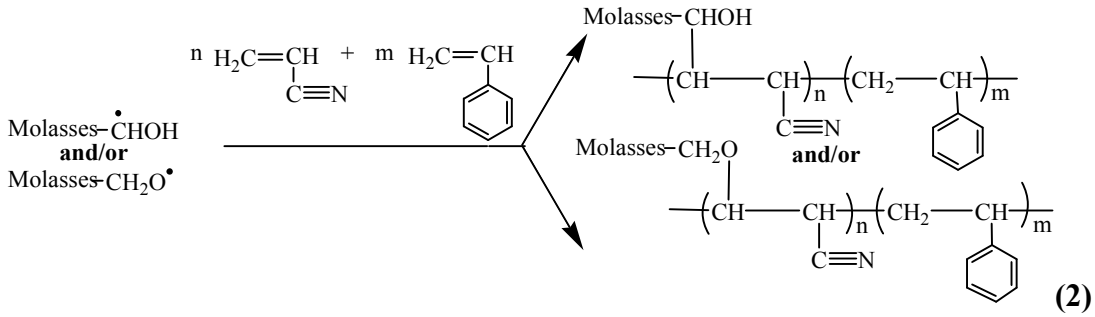

(2)

Interest in hybridizing clays into polymers at the nanoscale level is intense due to the pronounced improvements in properties at surprisingly low clay contents. Layered smectite-type montmorillonite (Mt) is a hydrous alumina silicate mineral which adsorbs cations such as K^{+}, Na^{+}, Ca^{+2} and Mg^{+2}. NaMt was used in the synthesis of clay nanocomposites of monosaccharide-mediated poly(styrene-*co*-acrylonitrile) (MSAN/NaMt) in this study. 0,5% (MSAN/NaMt80); 1% (MSAN/NaMt81); 1,5% (MSAN/NaMt82) and 2% (MSAN/NaMt83) NaMt containing composite samples were synthesized by in situ polymerization.

Structure of products were identified by FT-IR and ^{1}H-NMR analysis. Results of these analysis demonstrated the formation of desired products. XRD analysis was performed to determine interactions between NaMt and MSAN. In the results of XRD analysis, no diffraction peak (d_{001}) was observed in composite samples. It is decided it may be caused by the totally dispersion of NaMt layers or the covering of NaMt with polymer. Rheology measurements were performed to determine flow behaviours of products. According to the rheology measurements, MSAN78 and MSAN/NaMt samples displayed rheopectic behaviour. MSAN78 displayed Bingham plastic model while MSAN/NaMt samples displayed pseudoplastic behaviour. After addition of NaMt, some changes in rheological properties were observed. Appearent viscosity increased with shear rate due to the increase of number of NaMt particles in the dispersion. Thermal behaviour and enhancement in thermal stability of MSAN78 and MSAN/NaMt samples were observed by DSC and TGA analysis. According to the DSC analysis, MSAN78 and MSAN/NaMt samples, displayed two glass transitions. Melting and decomposition temperatures were determined from DSC thermograms and an obvious increase was observed in melting and decomposition temperatures by increase amount of NaMt. According to the TGA analysis, decomposition temperatures of MSAN/NaMt samples, demonstrated an increase by increasing of NaMt percent compared to MSAN78. Thermal analysis demonstrated the enhancement in thermal stability which NaMt provided in nanocomposites. DMA analysis was performed to determine mechanical resistance of MSAN78 and MSAN/NaMt samples. According to the Young's modulus values, elasticity of MSAN/NaMt samples increased by the increase of NaMt percent. When the breaking points were observed, it has seen that the rupture of MSAN78 film occurs in the lowest stress and strain values. DMA analysis demonstrated the enhanced mechanical resistance of MSAN/NaMt samples compared to MSAN78. Water sorption test was performed to determine water sorption of MSAN78 and MSAN/NaMt samples and the enhancement in water resistance by the increase of NaMt percent. MSAN78 had the most water sorption while water sorption of MSAN/NaMt samples decreased by increasing amount of NaMt. It is obvious that NaMt provided a good water resistance to MSAN78.

ŞEKER PANCARI YAN ÜRÜNÜNDEN POLİMER/KİL NANOKOMPOZİT ELDESİ

ÖZET

Şeker pancarı melası, şeker üretiminin başlıca yan ürünüdür. Melas, suyun yanı sıra rafinoz, glukoz, fruktoz ve ayrıştırılmamış sakkaroz gibi indirgen şekerler ve monosakkaritler dışındaki bazı maddeleri içerir. Melasın şeker içeriği %46-48 olarak kabul edilmektedir. Melas en fazla çiftlik hayvanlarının beslenmesinde katkı maddesi olarak kullanılır.

Poli(stiren-*ko*-akrilonitril) (SAN), stiren ve akrilonitril monomerlerinin kopolimeridir. Sertlik, saydamlık ve termal kararlılık gibi özelliklerinden dolayı SAN kopolimerleri endüstride yaygın olarak kullanılmaktadır. Çoğunlukla ev aletleri, elektrikli aletler, otomobil ekipmanları, bulaşık makinaları, buzdolapları, elektrikli süpürgeler, nemlendirici cihazlar gibi endüstriyel ve ev gereçlerinde yada bunların bazı parçalarında kullanılmaktadır. SAN ayrıca cam elyafı ile güçlendirilerek gösterge panellerinde ve akü kaplarında kullanılmaktadır.

Bu çalışmada; rafinoz, glukoz, fruktoz ve ayrıştırılmamış sakkaroz gibi monosakkaritler içeren melas, stiren ve akrilonitrilin polimerleşmesinde kullanılarak değerlendirilmiştir. Monosakkaritler, alkol grupları içeren bileşiklerdir. Monosakkarit molekülü ile Ce(IV) kompleks oluşturarak serbest radikal meydana getirirler (1). Melas, Ce(IV)'ü Ce(III)'e indirgeyen indirgen ajan görevi görür.

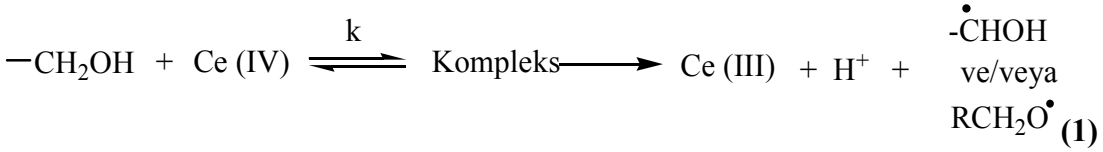

(1)

Bu şekilde, polimerizasyonu başlatmak üzere, monosakkaritler üzerinde serbest radikaller oluşturulmuştur (2). Monosakkarit temelli poli(stiren-ko-akrilonitril) (MSAN), emülsiyon polimerizasyonuyla sentezlenmiştir. En uygun reaksiyon koşullarını belirlemek üzere deneyler yapılmıştır. Bulunan uygun reaksiyon koşulları (MSAN78), polimer-kil nanokompozitlerinin sentezlenmesinde de uygulanmıştır.

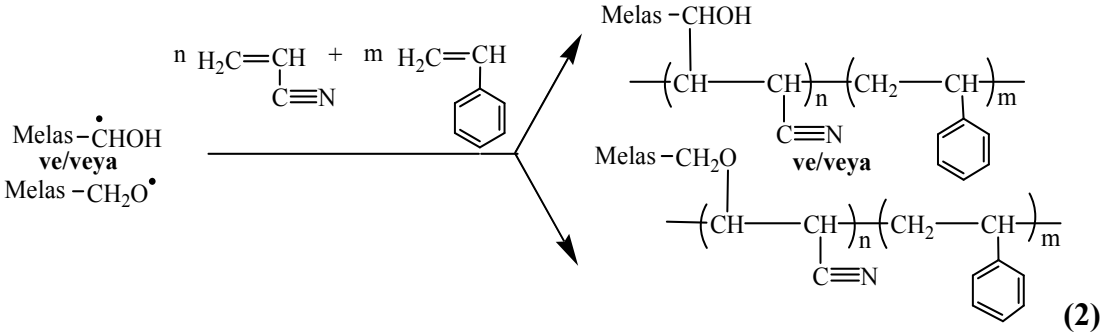

(2)

Çok düşük kil miktarlarıyla bile polimerlerin özelliklerine belirgin gelişmeler kazandırması nedeniyle, nano düzeyde polimer-kil etkileşimleri yoğun ilgi çekmektedir. Katmanlı smektit tipi olan montmorillonit (Mt), K^{+}, Na^{+}, Ca^{+2} and Mg^{+2} gibi katyonları yüzeyinde adsorplayabilen, bir su tutan alümina silikat mineralidir. Bu çalışmada, monosakkarit temelli poli(stiren-ko-akrilonitril) kil nanokompozitlerinin (MSAN/NaMt) sentezlenmesinde NaMt kullanılmıştır. 0,5% (MSAN/NaMt80); 1% (MSAN/NaMt81); 1,5% (MSAN/NaMt82) ve 2% (MSAN/NaMt83) NaMt içeren kompozit örnekleri in situ polimerizasyon metoduyla sentezlenmiştir.

Elde edilen ürünlerin yapıları FT-IR ve ^{1}H-NMR analizleriyle aydınlatılmıştır. Bu analizlerin sonuçları istenen yapıların oluştuğunu göstermiştir. NaMt ile MSAN arasında oluşan etkileşimleri belirlemek için XRD analizleri yapılmıştır. XRD analizi sonuçlarına göre, kompozit örneklerinin analizlerinde difraksiyon piki (d_{001}) gözlenmemiştir. Bunun nedeninin kilin çok iyi dağılmış olması yada kilin polimer tarafından kaplanmış olması olduğu düşünülmüştür. Elde edilen ürünlerin akış davranışlarının belirlenmesi amacıyla Reoloji analizi yapılmıştır. Reoloji sonuçlarına göre, MSAN78 ve MSAN/NaMt örnekleri reopektik davranış göstermiştir. MSAN/NaMt örnekleri psödoplastik davranış gösterirken, MSAN78 Bingham plastik davranış göstermiştir. NaMt eklenmesiyle beraber, reolojik özelliklerde bazı değişimler gözlenmiştir. Kayma hızı artışıyla beraber görünür viskozite, NaMt partiküllerinin yüzdesinin artmasıyla artış göstermiştir. MSAN78 ve MSAN/NaMt örneklerinin termal davranış ve termal dayanımlarının incelenmesi DSC ve TGA analizleriyle gerçekleştirilmiştir. DSC analizi sonuçlarına göre, MSAN78 ve MSAN/NaMt örnekleri iki camsı geçiş gerçekleştirmiştir. DSC termogramlarında gözlenen erime ve bozunma sıcaklıkları, artan NaMt miktarıyla, artış göstermiştir. TGA analizi sonuçlarına göre ise, MSAN/NaMt örneklerinin bozunma sıcaklıkları, MSAN78'e kıyasla, artan NaMt miktarıyla beraber artış göstermiştir. Termal analiz sonuçları, NaMt'nin termal kararlılıkta gelişme sağladığını göstermiştir. MSAN78 ve MSAN/NaMt örneklerinin mekanik dayanımlarının incelenmesi için DMA analizleri gerçekleştirilmiştir. Elastikiyet katsayısı değerlerine göre, MSAN/NaMt örneklerinin elastikliğinin NaMt yüzdesi arttıkça arttığı gözlenmiştir. Kopma noktaları incelendiğinde ise MSAN78 filminin en önce koptuğu görülmüştür. DMA analizi MSAN/NaMt örneklerinin MSAN78'e kıyasla mekanik özelliklerinin geliştirilmiş olduğunu göstermektedir. MSAN78 ve MSAN/NaMt örneklerinin su tutma özelliklerinin incelenmesi ve suya karşı dayanımdaki gelişmeyi gözlemlemek için, su tutma testi gerçekleştirilmiştir. MSAN/NaMt örneklerinin su tutması içerdikleri kil yüzdeleri arttıkça azalma gösterirken, en fazla suyu MSAN78 tutmuştur. Burdan da NaMt'nin polimere suya karşı iyi bir dayanım kazandırdığı görülmüştür.

1. INTRODUCTION AND AIM

In recent years, polymer-clay nanocomposite systems carry on their importance and popularity due to the enhancement that they provide to the polymeric materials. They provide improvement such as in mechanical strength, modulus, thermal stability, gas barrier properties, fire-retardant properties, corrosion resistance, ionic conductivity and decreased absorption in organic liquids.

Poly(styrene-*co*-acrylonitrile) SAN is a copolymer of acrylonitrile and styrene monomers. It has more advantages than polystyrene or polyacrylonitrile homopolymers due to its better chemical and physical properties [1]. It has many application area such as dials, knobs, and covers for domestic appliances, electrical equipment, car equipment, dishwasher safe housewares, such as refrigerator meat and vegetable drawers, blender bowls, vacuum cleaner parts, humidifier parts, plus other industrial and domestic applications with requirements more stringent than can be met by polystyrene.

In this study, synthesis of SAN and NaMt nanocomposites of SAN was performed because of its appropriate chemical/physical properties and wide application area. During the synthesis of SAN and SAN-NaMt nanocomposites, sugar beet molasses was used as reducing agent because of its content of reducing monosaccharides (raffinose, glucose, fructose and unseperated sucrose etc.) in various amounts. Sugar beet molasses is a by-product of sugar production. It has a number of application area generally as a component in compound feeds, livestock feeds and silage additives. Utilization of molasses as a reducing agent in radicalic redox polymerization is thought to be an alternative application area.

This study has two main goals. One of them is to investigate preparation of monosaccharide-mediated SAN (MSAN) by radicalic redox polymerization and preparation of its nanocomposites by in situ methods and finally to characterize and compare polymers and nanocomposites in terms of their thermal, mechanic, rheological and water sorption properties. The other aim is to utilize sugar beet molasses which is a by-product.

2. THEORETICAL PART

2.1 Molasses

Molasses (Figure 2.1) is primarily a by-product of sugar production, but not always [2]. Most comes from sugar cane, but also sugar beets, citrus, starch and wood. Molasses from cane and beets are a by-product of sugar production. Starch molasses is a by-product from the manufacture of glucose from cornstarch. Wood starch molasses (also lignin sulfonate or hemicellulose extract) is a by product from the manufacture of pressed woods and wood pulp.

Figure 2.1 : Sugar beet molasses

All molasses are categorized according to Brix, correlation to density. The molasses trade commonly use the term Brix as an indicator of specific gravity and represents an approximation of total solids content. Brix is a term originally initiated for pure sucrose solutions to indicate the percentage of sucrose in solution on a weight basis. For example, 25 Brix means 25 g sucrose/100 g solution or 25 g sucrose/75 g water. However, in addition to sucrose, molasses contains glucose, fructose, raffinose and numerous non-sugar organic materials. Consequently, a Brix value for molasses will often differ dramatically from actual sugar or total solid content [3]. Most molasses products are between 67-78% dry matter (22-33% moisture), dehydrated 94-95% dry matter (more expensive) [2].

There are three major types of cane molasses: unsulphered, sulphured and blackstrap molasses [3]. There are also three major grades of cane molasses: first molasses, second molasses, and blackstrap molasses.

When sugar cane plant is harvested, the leaves are stripped. The juice is extracted from the cane by crushing or mashing, boiled to remove most of the water, and later processed to extract the sugar. The results of this first boiling and processing is first molasses, which has the highest sugar content because comparatively little sugar has

been extracted from the juice. Unsulphered molasses is the finest quality. It is made from the juice of sun-ripened cane and the juice is clarified and concentrated. Barbados molasses is one type of unsulphered molasses, light in colour and high in sucrose mainly sold for cooking, confectionery and in the production of rum.

Second molasses is created from a second boiling and sugar extraction, so there is less sugar. It has a darker colour and a slightly bitter taste, or as some would say a more pronounced flavour.

Further rounds of processing and boiling yield blackstrap molasses. Blackstrap molasses is from the third boil and has a commercial value in the manufacture of cattle feed and other industrial uses. It is 55 to 65% sugar.

Sulphured molasses is made from green sugar cane that has not matured long enough and treated with sulphur fumes during the sugar extracting process.

Cooking molasses is a blend of fancy and blackstrap molasses. It is 59 to 69% sugar.

Cane molasses is a by-product of the manufacture or refining of sucrose from sugar cane. Cane molasses purchased as an animal feed will contain more than 46% total sugars expressed as invert sugars. If its moisture content exceeds 27%, its density determined by double dilution must not be less than 79,50 Brix.

Beet molasses is a by-product of the manufacture of sugar (sucrose) from sugar beets. It will have more than 48% total sugars expressed as invert and its density determined by double dilution must not be less than 79,50 Brix.

However, some molasses from sugar beets is so well processed it has virtually no sugar. So, if you are buying beet molasses, be sure to find out first if it is sweet. Citrus molasses is the partially dehydrated juices obtained from the manufacture of dried citrus pulp. It must contain not less than 45% total sugars expressed as invert and its density determined by double dilution must not be less than 71,0 Brix.

Starch molasses is a by-product of dextrose manufacture from starch derived from corn or grain sorghums where the starch is hydrolyzed by enzymes and/or acid. It is at least 43% reducing sugars expressed as dextrose and not less than 50% total sugars expressed as dextrose.

Interestingly, molasses is also an excellent chelating agent. An object coated with iron rust placed for two weeks in a mixture of one part molasses to nine parts water will lose its rust due to the chelating action of the molasses.

2.1.1 Sugar beet molasses

Molasses that comes from the sugar beet is different from cane molasses [4]. Only the syrup left from the final crystallization stage is called molasses; intermediate syrups are referred to as "high green" and "low green" and these are recycled within the crystallization plant to maximize extraction. Beet molasses is about 46-48% sugar by dry weight, predominantly sucrose but also containing significant amounts of glucose and fructose. Beet molasses is limited in biotin (Vitamin H or B_7) for cell growth, hence it may need to be supplemented with a biotin source. The non-sugar content includes many salts such as calcium, potassium, oxalate, and chloride. These are either as a result of concentration from the original plant material or as a result of chemicals used in the processing. As such, it is unpalatable and is mainly used as an additive to animal feed (called "molassed sugar beet feed") or as a fermentation feedstock.

It is possible to extract additional sugar from beet molasses through a process known as molasses desugarisation. This technique exploits industrial scale chromatography to separate sucrose from non-sugar components. The technique is economically viable in trade protected areas where the price of sugar is supported above the world market price. As such it is practiced in the U.S.

Beet molasses is included in animal feed, alcohol, beverages, bakery goods and pharmaceuticals [5].

Molasses is produced as a by-product during the production process of sugar from sugar beet in many factories in Turkey. The production 2007-2008 term total molasses production is 269.300 tones in Turkey [6]. Molasses production in Turkey is given in detail in Table 2.1.

Table 2.1: Molasses production in respect of factories in Turkey

Factory	Molasses (Tones)	Factory	Molasses (Tones)
Afyon	15.040	Erzurum	7.928
Ağrı	6.492	Eskişehir	22.178
Alpullu	7.016	Ilgın	20.885
Ankara	12.600	Kars	3.035
Bor	9.607	Kastamonu	8.500
Burdur	13.700	Kırşehir	8.044
Çarşamba	5.830	Malatya	8.176
Çorum	15.021	Muş	7.440
Elazığ	5.506	Susurluk	13.530
Elbistan	7.533	Turhal	23.345
Erciş	3.678	Uşak	5.240
Ereğli	25.980	Yozgat	7.070
Erzincan	5.926	**Total**	269.300

2.1.2 Content of sugar beet molasses

Most molasses products are between 67-78% dry matter (22-33% moisture), dehydrated 94-95% dry matter (much more expensive)[2].

2-6% crude protein, low in vitamins A, D, B1 and B2, but are a good source of pantothenic acid and niacin. Energy content 3,4-3,5 Mcal/kg, similar to oats, but energy in molasses is in the form of monosaccharides/simple sugars, primarily sucrose, fructose and glucose; while energy in grains is primarily in the form of starch.

Molasses is known to be containing organic acids such as mainly lactic acid (1.7%), malic, fumaric, valeric, oxalic acids and the trace amount of glucuronic and galactronic acids where the total organic acid content can reach up to 4% [7]. Potassium, calcium, magnesium and sodium constitute a wide percentage of molasses and it is stated that ferrum, zinc, manganese, copper, cobalt and lead are present in trace amounts in molasses. Beside water, fermentable monosaccharides (sucrose, glucose, fructose), the materials except monosaccharides and the materials generated during the process and storing constitute the composition of molasses. The

sugar content accepted for sugar beet molasses is 46-48%. Also, it is determined that the materials acting as inhibitor and increasing fermentation are present in molasses. The content of sugar beet molasses comparable with cane molasses types are shown in the Table 2.2 [8].

Table 2.2: Analysis of molasses types

Content	Standart cane Molasses (%)	Feed cane Molasses (%)	Sugar beet Molasses (%)
Dry matter	73	71	73
Water	27	29	27
Total sugars	44-47	42-44.5	46-48
Crude protein	3-5	3-5	8-10
Crude ash	8-12	8-12	8-10
Crude fiber	0	0	0
Crude oil	0	0	0
Calcium	0.8	0.7	0.5
Phosphorus	0.5	0.4	0.3
Potassium	3	2.9	4
Magnesium	0.3	0.2	0.09
Copper	7-15*	7-15*	11*

*ppm

2.1.3 Industrial application of sugar beet molasses

Due to its unique physical and chemical properties molasses has traditionally been used as a major component in compound feeds, livestock feeds and silage additives [9]. However, it is now also being more widely used in various industrial processes.

Molasses has recently been recognised in a number of different industries, including food and drinks manufacture, fuels, rubber, printing, chemical and construction industries, alongside the traditional agricultural uses.

Animal feeding

Molasses is mainly used in animal feeding [2]. It is added to livestock rations for four reasons:

- increases palatability.
- reduces dustiness of feed in processing (remember risk of explosions in grain mills).
- binder in pelleting or to keep loose particles of feed (ie vit/min premix) from sifting out.
- sometimes used as a carrier for a mineral or protein source (such as urea) provided as a lick to range cattle.

It is high in reducing agents which have an effect on lysine, research reported destruction of 0,5% lysine content per day. So if molasses is in grain mix, 1/3 of lysine content would be destroyed within 3 months and 1/2 of lysine content would be destroyed within 5 months. It does not mean to not use molasses in grain mix, just means to either feed grain quickly, supply additional lysine, or don't feed grain mixes with a lot of molasses to young, growing animals.

Molasses is usually added to grain as 5% of the total mixture. More than 5% in loose grain mix in hot, humid weather may lead to mold, and more than 10% makes it too sticky and hard to handle. When used as a binder in pelleting, molasses usually added between 7-10%. All molasses products have a laxative effect and rations more than 15-25% cause diarrhea and digestive upset.

Palatability differs among different types of molasses. Cane molasses has the most pleasing odor and is the most palatable, this is the one used for human consumption (blackstrap molasses). Beet molasses has a fishy odor, but doesn't affect palatability for livestock. Cattle like wood molasses the least, and pigs like citrus molasses the least.

Binding

Its main advantage over traditional binding materials is that it does not release pollutants, during high temperature manufacture [9]. When molasses is burned it produces only carbon dioxide and water. In contrast, other traditional binding agents produce toxic emissions on combustion.

Coal Briquettes

Molasses is an environmentally friendly binding agent for coal briquettes for domestic and industrial use.

Carbon Black Agglomeration

Industrial molasses provides a consistent and stable performance as a binding agent for more efficient and safer handling of this fine powder which is used to reinforce and colour pneumatic tyre rubber and employed in printing pigments, sugar refining and other chemical processes.

Stabilising Cement

A low rate of molasses, added to cement, delays concrete setting by 12-24 hours. This allows pumping or temporary storage, which is very beneficial for large scale operations such as motorway construction.

Jumadurdiyev et al. studied [10] about usage of molasses in delaying hardening of cement. Molasses, a by-product of sugar industry, increases the fluidity of fresh concrete, and also delays the hardening time of cement paste. Setting times of cement pastes prepared with molasses at three different dosages (0,20, 0,40, and 0,70 wt.% of cement content) were determined and it was found that molasses addition causes considerable increase in both initial and final setting times. Flexural and compressive strengths were determined on hardened concretes at both early ages (1, 3, and 7 days), and moderate and later ages (28, 90, 180, 365, and 900 days).The strength of concretes with molasses showed slight increase at all ages, except early age, with respect to the control mix and no adverse effect has been experienced on the durability properties over a long period of time (900 days).

Casting Moulds

Molasses makes an effective sand glue for casting moulds. The lack of toxic emissions during firing and moulding gives it a distinct advantage over more conventional substances.

Fermentation Processes

Molasses is used as an energy source in a wide range of fermentation processes to grow yeasts, moulds and bacteria which produce brewing, baking, distilling and feed yeasts [9].

Bakers and Brewers Yeasts

Molasses has a significant biotin content needed for growth in bakers and brewers yeast.

Citric Acid

Large amounts of citric acid for soft drinks and pharmaceuticals manufacture are produced from moulds adapted to utilise molasses as their energy source.

Industrial Alcohol

Industrial molasses contains B Vitamins and biotin, both helpful in the fermentation process to produce alcohol for use in alcohol drinks, cosmetics and solvents. Beet molasses due to its buffering capacity requires a higher content of sulphuric acid to reduce pH to optimum fermentation levels than when cane molasses forms the energy source.

Lotfy studied [11] the utilization of beet molasses as a novel carbon source for cephalosporin C production by Acremonium Chrysogenum. Under experimental conditions; Soya oil, beet molasses and corn steep liquor were found to be the major factors contributing to the antibiotic production.

M.S.G.(Monosodium glutamate) & Lysine

Molasses is the perfect energy source for the complicated technology involved in producing M.S.G. and Lysine. These amino acids are increasingly used in human and livestock food processing. Only can molasses provides the biotin required for both processes.

Food Products

The high energy and digestibility characteristics of molasses allied to an attractive taste and aroma, make it an increasingly used constituent of human food products [9]. Molasses is used as a flavouring and colouring agent, in sauces, speciality sugars, brown sugars and sweets. It is also incorporated into specialist compost which provides a high energy activator for mushrooms.

Palatability differs among different types of molasses. Cane molasses has the most pleasing odor and is the most palatable, this is the one used for human consumption (blackstrap molasses). Beet molasses has a fishy odor, but does not affect palatability for livestock [2].

Additionally, there are studies to utilize molasses for alternative application areas. Yang et al. [12] studied the alkaline degradation of invert sugar from molasses to be used as de-icer. Sugar beet and sugar cane molasses have shown to be suitable

starting materials for producing de-icer preparations. The sucrose in the molasses hydrolyzed to glucose and fructose by invertase. The reducing sugars then degraded by NaOH, the alkali neutralized by the sugar acids produced, resulting in an increase of the ionic strength and consequently depression of the freezing point of the resulting solution. The reaction products showed the same freezing point depression as seen in the degradation products from pure glucose.

2.2 Properties and Usage of Ce(IV) in Redox Polymerization

Ce(1V) ions are versatile reagents for the oxidation of numerous functional groups in organic synthesis, as well as in transition metal chemistry [13]. They are also employed to achieve nitration, hydroxylation, rearrangement, addition of carbonyl compounds to 1,3-dienes, homolytic malonylation of aromatic hydrocarbons, alkoxyiodination, nitratoiodination, and more. Most of these transformations open up a broad applicability due to their mild reaction conditions, fast conversions, and convenient work-up procedures. The use of ceric ion as an oxidant for organic substrates gained prominence as an analytical reagent. Most of the reactions involve a direct oxidation of the organic compound by Ce(1V). However, some indirect oxidations are also considered in which Ce(1V) produces an active oxidant.

2.2.1 Oxidations of Ce(IV)

Cerium is a member of Group III A of the periodic table, commonly referred to as rare earth metals, lanthanons, or lanthanides [14]. The normal oxidation states of cerium salts are three (cerous, Ce(III)) and four (cerium, Ce(IV)); therefore, monomeric cerium will be a one-electron oxidant. Cerous compounds resemble other trivalent lanthanons, but cerium compounds are like the elements titanium, zirconium, and thorium. The oxidation potential for the reaction (2.1), depends on the nature of the medium.

$$Ce(III) \rightleftharpoons Ce(IV) + e^- \qquad \textbf{(2.1)}$$

Values of E^0_{298} are reported to be between -1.28 and -1.70 V. The electrode potential for the reaction (2.2), is +2,335 V on the hydrogen scale.

$$Ce(s) \rightleftharpoons Ce(III) + 3e^- \quad \textbf{(2.2)}$$

Principal advantages of employing Ce(IV) as an oxidizing agent are;

- There is only one oxidation state, Ce(III), to which the Ce(IV) ion is reduced, and the redox potential of the Ce(IV)/Ce(III) couple is high.
- It is a very powerful oxidizing agent and, as mentioned above, one could alter the intensity of its oxidizing power by suitable choice of the medium.
- Oxidation by Ce(IV) proceeds in one step (2.3).

$$Ce(IV) + e^- \rightleftharpoons Ce(III) \quad \textbf{(2.3)}$$

- Acid solutions of Ce(IV) ions are extremely stable. Solutions can be kept for an indefinite period of time without any change in their concentration.
- Ce(IV) solutions could be employed, even in the presence of chloride ion, for oxidations that must be carried out by the use of excess reagent at elevated temperatures. However, chloride ion becomes oxidized when the solution is boiled.

2.2.2 Theory of oxidations involving intermediate complexes

With the exception of one reported study [15] Ce(IV) oxidations of organic substrates are generally believed to involve direct transfer of a single electron. It seems reasonable that the reaction mechanism will include an interaction between the Ce(IV) and the organic substrate. Two types of mechanisms can be distinguished depending on the nature of this interaction. In the first mechanism a stable coordination complex is formed between the Ce(IV) and the organic substrate, R, in a rapid preliminary equilibrium step. The intermediate complex then disproportionates, unimolecularly, in the rate-determining step forming Ce(III) and a free radical $R^{\bullet}$ (2.4).

$$Ce(IV) + R \overset{K}{\rightleftharpoons} Complex \xrightarrow[slow]{k} Ce(III) + R^{\bullet} + H^+ \quad \textbf{(2.4)}$$

Free radical is rapidly oxidized by a second mole of Ce(IV) (2.5):

$$Ce(IV) + R^{\bullet} \xrightarrow{\text{fast}} Ce(III) + \text{Product} + H^{+} \qquad \textbf{(2.5)}$$

The second mechanism assumes that the substrate is oxidized directly by Ce(IV). In this case the interaction takes place in the transition state (2.6):

$$Ce(IV) + R \longrightarrow [Ce(IV)\text{-------}R] \longrightarrow Ce(III) + R^{\bullet} + H^{+} \qquad \textbf{(2.6)}$$

As in the first mechanism (2.4), the free radical is rapidly oxidized by a second mole of Ce(IV). The participation of intermediate complexes in the reaction mechanism can be evaluated from kinetic data. Duke [16] originally derived the general theory for oxidations involving intermediate complexes and was the first to apply it to Ce(IV) oxidations. It is assumed: (1) that the stoichiometry of the complex requires one oxidant and one substrate molecule (2.4); (2) that coordination equilibrium is rapidly established and that equilibrium is maintained despite the unidirectional disproportionation of the complex; and (3) the free radical formed is rapidly oxidized by a second mole of Ce(IV) (2.5).

Free radicals are produced from two types of complexes, alcohol complex and the glycol complex, as shown in (2.6), where A and B are alcohol and glycol complexes, respectively.

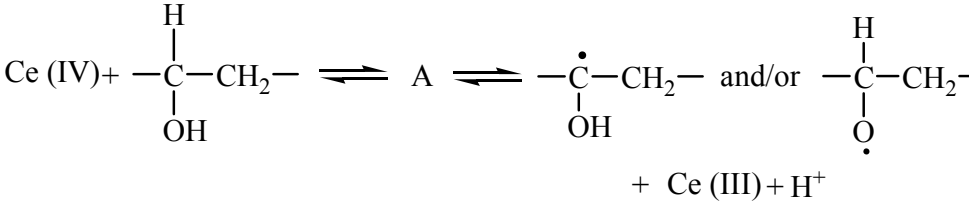

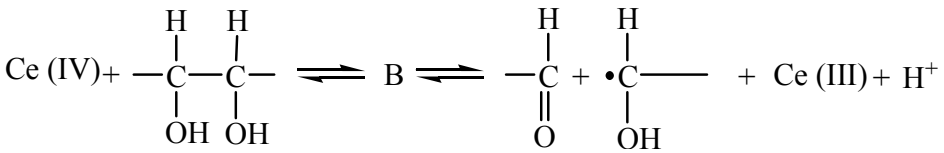

(2.7)

2.2.3 Synthesis of block and graft copolymers by Ce(IV) initiated redox polymerization

The possibility of modifying cellulosic materials by graft copolymerization with vinyl monomers has directed research effort to various methods of generating free radicals. The cerium ion-alcohol redox system, suggested by Mino and Kaizerman [17], has received much attention. The mechanism of free radical formation is believed to involve the formation of a complex between cerium ion and cellulosic hydroxyl groups. The complex then disproportionate unimolecularly forming a free radical on the cellulose backbone. The free radical initiates polymerization when vinyl monomers (M), are present. The mechanism can be summarized as (2.8):

$$\mathrm{Ce(IV) + ROH \rightleftharpoons Complex \longrightarrow Ce(III) + H^{+} + \dot{R}OH}$$

$$\mathrm{\dot{R}OH + M \longrightarrow R(OH)M^{\bullet}}$$

$$\mathrm{R(OH)M^{\bullet} + nM \longrightarrow R(OH)M_{n+1}} \qquad \textbf{(2.8)}$$

The polymerization is terminated by oxidation of the free radical by Ce(IV).

For initiating vinyl polymerization Ce(IV) ions are used alone or in conjunction with suitable reducing agents [18]. Various alcohols such as benzyl alcohol, ethanol, ethylene glycol, and 3-chloro-1 propanol have been employed with cerium ions to form redox systems for homopolymerization, block or graft copolymerization.

Pramanick and Sarkar [19], investigated the polymerization of methyl methacrylate initiated by only cerium ions and found that the mechanism of initiation depends strongly on the acidity of the medium and is independent of the nature of anion associated with the cerium ion. In a moderately acidic medium, the primary reaction is the formation of hydroxyl radical by cerium-ion oxidation of water. When cerium sulfate is used, the hydroxyl radicals initiate the polymerization and appear as end groups in the polymer molecule. If, on the other hand, cerium ammonium sulfate or a mixture of cerium sulfate and ammonium sulfate are used, some of the hydroxyl radicals react with the ammonium ion, producing ammonium radicals, and both radicals act as initiators, giving polymers with both hydroxyl and amino end groups.

Ce (IV) salts are well known initiators for graft copolymerization of vinyl monomers such as acrylonitrile and acrylamide. For example, a redox reaction between Ce(IV)

and -CH_2OH groups of ketonic resin and free radicals generated initiates the polymerization (2.9) [20].

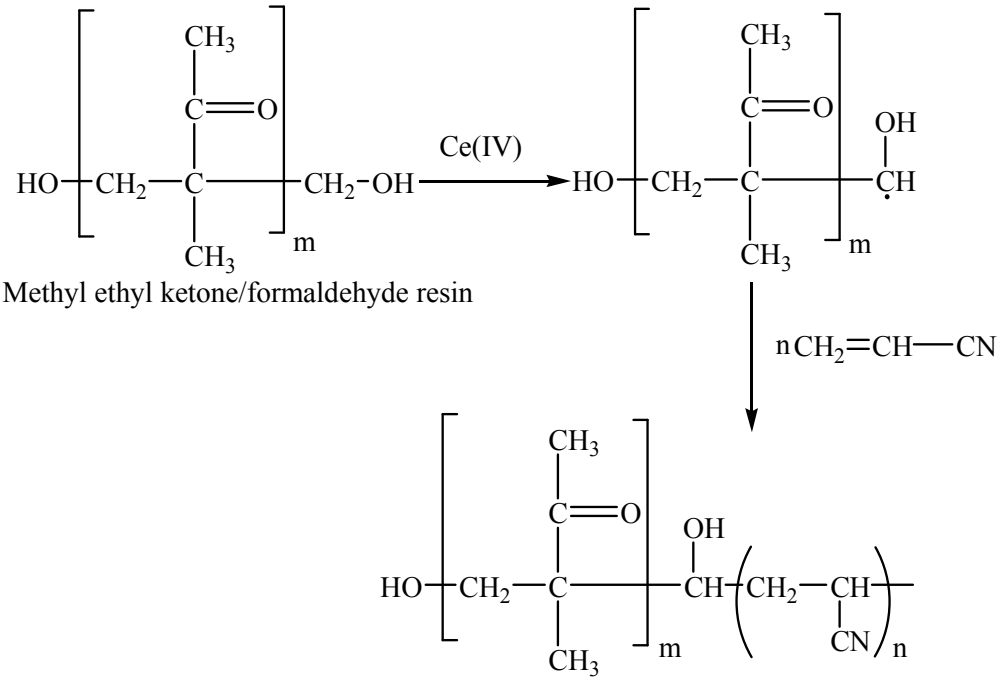

(2.9)

In the first step, Ce(IV)/methylol redox reaction occurs and free radicals are generated. These free radicals initiate polymerization of acrylonitrile. Polymerization may proceed from other –CH_2OH groups of ketonic resin molecule also. This occurs when Ce(IV) (linear termination) or combination by themselves (mutual termination) may both be possible, by depending on the Ce(IV) concentration. Increasing Ce(IV) concentration results in a linear termination.

Water-soluble cellulose derivatives such as methyl cellulose (MC) and methyl hydroxy propyl cellulose (MHPC) (2.10) and polyethylene glycols (2.11) were also used as reducing agents for block/graft copolymer synthesis of acrylamide and acrylonitrile [21].

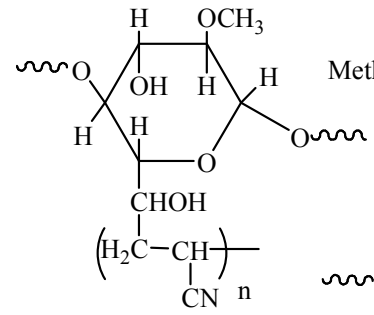

Methyl Celulose-polyacrylonitrile (MC-PAN)

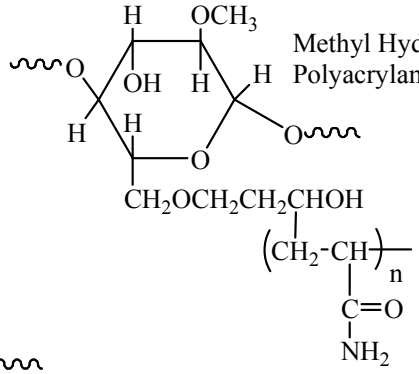

Methyl Hydroxypropyl Cellulose-Polyacrylamide (MHPC-PAM)

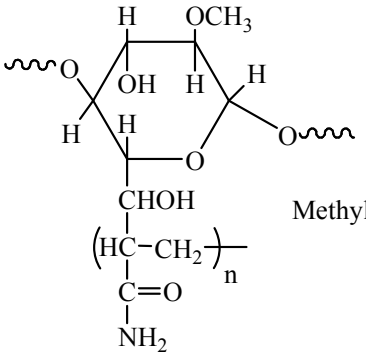

Methyl Celulose-polyacrylonitrile (MC-PAM)

(2.10)

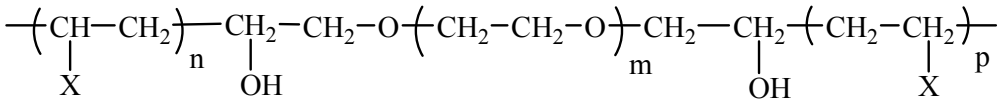

m= 30 and 90

X= CN, $CONH_2$ **(2.11)**

The redox system of a cerium salt and α,ω-dihydroxy poly(dimethylsiloxane) is used by Öz and Akar [22] to polymerize vinyl monomers such as acrylonitrile and styrene to produce block copolymers (2.12).

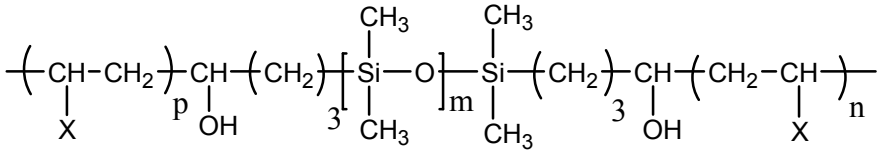

(2.12)

The concentration and type of α,ω-dihydroxy poly(dimethylsiloxane) has shown to affect the yield and molecular weight of the copolymers. The copolymers obtained have lower glass-transition temperatures at about 208ºC and much higher contact angle values than those of the corresponding homopolymer of vinyl monomers,

regarding the fact that the weight percentage of α,ω-dihydroxy poly(dimethylsiloxane) of the copolymers was in the range of 1-2%.

Cerium ammonium nitrate in nitric acid has also been used to modify guar gum by the graft copolymerization of hydroxyethyl acrylate onto it [23]. A graft copolymer having 22% grafted chains with average degree of polymerization of side chains at 7300 was obtained. The Japanese patent [24] describes that the graft copolymer was obtained when 1 kg guar gum oxidized with H_2O_2 was dispersed in 5 L water containing 5 L methanol mixed with 300 g hydroxyethyl acrylate, 10 g cerium ammonium nitrate, and 1 mL 63% nitric acid, the reaction mixture was heated at 40-45°C for two hours. The overall reaction mechanism for graft copolymerization of vinyl monomers onto guar gum initiated by Ce(IV) ions may be represented in the scheme (2.13). Possible reaction mechanism proceeds on the complex formation of Ce(IV) and guar gum while guar gum radical and Ce(III) are being generated.

$$
\begin{aligned}
&GOH + Ce(IV) \longrightarrow Complex \\
&Complex \longrightarrow GO^{\bullet} + Ce(III) + H^{+} \\
&GO^{\bullet} + Monomer \longrightarrow Graft\ copolymer \\
&GO^{\bullet} + Ce(IV) \longrightarrow Products + Ce(III) + H^{+}
\end{aligned}
\qquad \textbf{(2.13)}
$$

where GOH is guar gum and $GO^{\bullet}$ is the guar gum radical.

Sharma, Kumar and Soni [25] investigated the graft copolymerization of acrylamide onto Cassia tora gum with cerium amonnium nitrate/nitric acid as the redox initiator. Complex formation between Ce(IV) and Cassia tora seed gum is shown in the **(2.14)**.

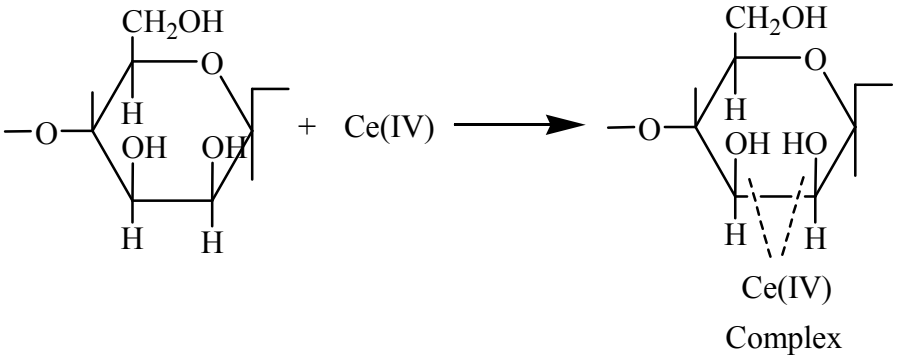

(2.14)

Proposed reaction mechanism of cerium ammonium nitrate-initiated graft copolymerization of acrylamide onto C. tora seed gum is represented in (2.15). Mechanism proposes the chain initiation, over complex between cerium ion and C. tora seed gum.

Chain initiation

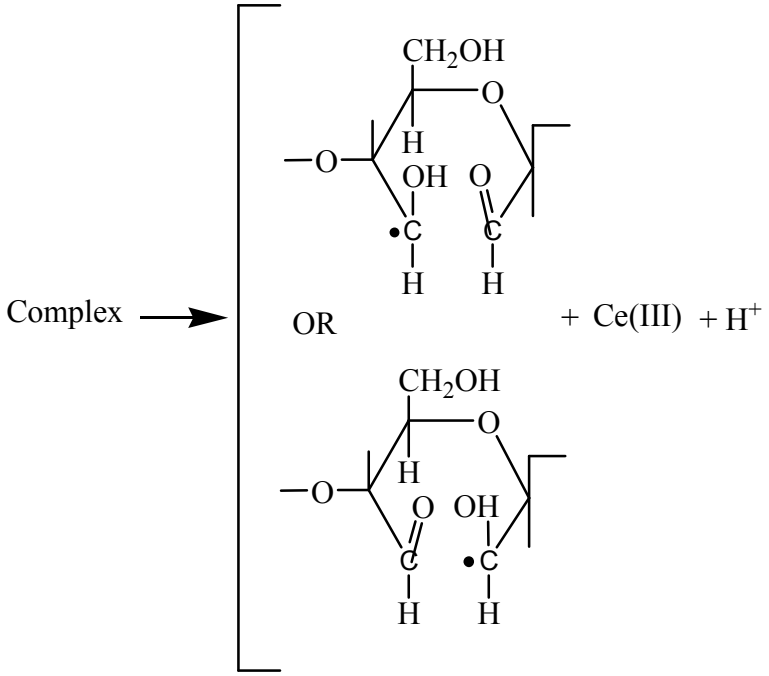

Chain propagation

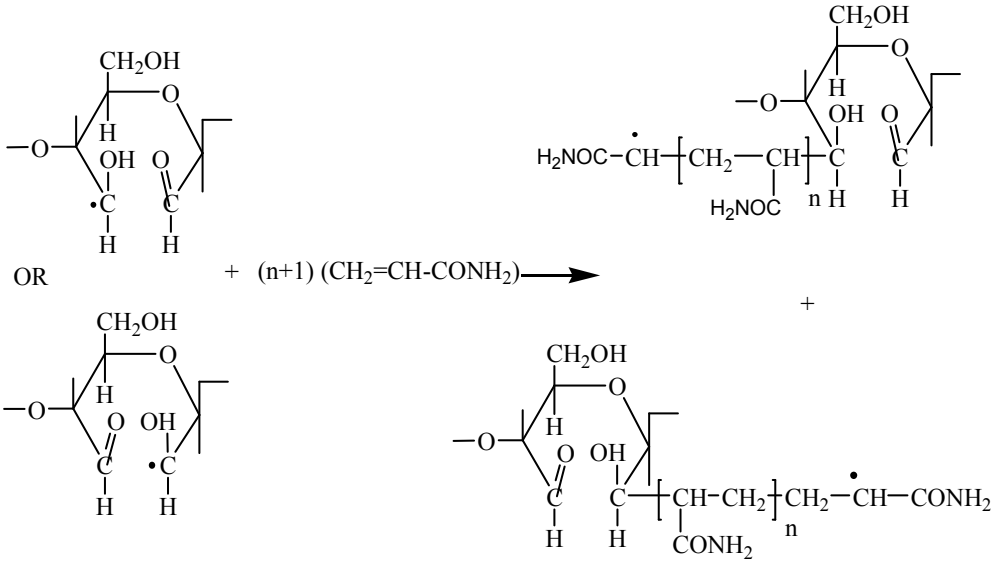

(2.15)

2.3 Poly(styrene-*co*-acrylonitrile) (SAN) Copolymer

Poly(styrene-*co*-acrylonitrile) is the copolymer of styrene and acrylonitrile monomers (2.16) [1].

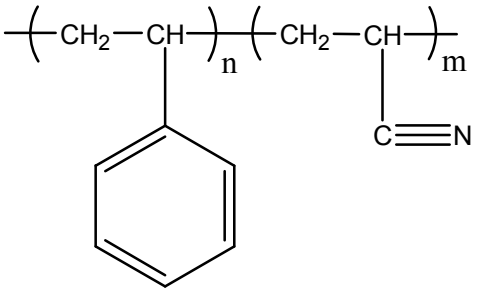

(2.16)

Because of the polar nature of the acrylonitrile molecule, SAN copolymers have better resistance to hydrocarbons, oils, and greases than polystyrene. These copolymers have a higher softening point, a much better resistance to stress cracking and crazing, and higher impact strength than the homopolymer polystyrene, in addition they retain the transparency. The toughness and chemical resistance of the copolymer increases with the acrylonitrile content but so do the difficulty in molding and the yellowness of the resin. Commercially available SAN copolymers have 20-30% acrylonitrile content. They are produced by emulsion, suspension, or continuous polymerization.

Due to their rigidity, transparency, and thermal stability, SAN resins have found applications for dials, knobs, and covers for domestic appliances, electrical equipment, car equipment, dishwasher safe housewares, such as refrigerator meat and vegetable drawers, blender bowls, vacuum cleaner parts, humidifier parts, plus other industrial and domestic applications with requirements more stringent than can be met by polystyrene. SAN resins are also reinforced with glass to make dashboard components and battery cases. Over 35% of the total SAN production is used in the manufacture of ABS blends.

SAN copolymers are amorphous, transparent, and glossy random copolymers produced by batch suspension, continuous mass (or solution), and emulsion polymerization processes [26]. The molecular weight and the acrylonitrile content of the copolymer are the key factors in determining polymer properties. SAN has improved tensile yield, heat distortion, and solvent residence than polystyrene because of the incorporation of acrylonitrile. For example, SAN is resistant to aliphatic hydrocarbons, alkalines, battery acids, vegetable oils, foods, and detergents.

SAN is attacked by some aromatic hydrocarbons, ketones, esters, and chlorinated hydrocarbons. Emulsion processes are used to produce SAN diluent for ABS resins. SAN produced by mass and suspension processes are primarily used for molding applications. A variety of copolymer properties or grades is available, depending on the molecular weight and the copolymer composition (styrene/acrylonitrile ratio).

The major problems in SAN processes are related to reactor temperature control, mixing, and copolymer composition control. The viscosities of concentrated SAN solutions are higher than polystyrene of the same molecular weight; thus, heat removal becomes more difficult. In a continuous reactor process, the mixing of low viscosity reacting fluid can be difficult. The polymerization rate is higher than that of styrene homopolymerization. If mixing is not homogeneous, SAN degrades resulting in coloring and contamination. To avoid composition drift in a batch copolymerization process, SAN copolymers are often manufactured at the azeotropic point, where monomer and polymer have the same composition (Figure 2.2). However, if the desired copolymer composition is not the azeotropic composition, the copolymer composition varies with conversion (or composition in the bulk phase). Composition drift in SAN copolymers is undesirable because SAN copolymers of different compositions are incompatible and cause phase separation. Therefore, it is very important to monitor the bulk-phase composition and to make some corrective actions to prevent the copolymer composition drift. For example, more reactive monomer or comonomer can be added to the reactor during polymerization to keep the monomer/comonomer ratio constant. The polymerization reactors that can be used for continuous mass processes are loop reactors and continuous stirred tank reactors (CSTR) with an anchor agitator.

2.3.1 Copolymerization of styrene and acrylonitrile

Styrene homopolymer is a brittle polymer [27]. Styrene copolymers are industrially of significant importance because a wide variety of polymer properties can be obtained by copolymerizing styrene with rubbers (diens) and other vinyl monomers. The copolymers of acrylonitrile and styrene are thermoplastics of increasing commercial importance because of their superior properties to those of polystyrene and the relative ease of fabrication [28]. The properties of SAN copolymers are dependent on their acrylonitrile content. With increasing acrylonitrile content,

copolymers demonstrate continuous improvements in barrier properties and chemical and UV resistance, but thermal stability deteriorates. These monomers exhibit strongly contrasting electron donating properties, and hence there is a strong tendency to alternation in copolymerization.

The copolymer composition can be determined by the reactivity ratios (2.17) defined as

$$r_1 = \frac{k_{11}}{k_{12}} \quad r_2 = \frac{k_{22}}{k_{21}} \tag{2.17}$$

The mole fraction (F_1) of monomer M_1 in the polymer phase can then be expressed as follows (2.18):

$$F_1 = \frac{r_1 f_1 + f_1 f_2}{r_1 f_1^2 + 2 f_1 f_2 + r_2 f_2^2} \tag{2.18}$$

where f_1 and f_2 are the mole fractions of monomer 1 and monomer 2 in the bulk phase, respectively. Figure 2.2 illustrates the copolymer composition curves for several styrene-comonomer systems. This Figure 2.2 shows that a high degree of composition drift and composition nonhomogeneity may occur in a styrene-acrylonitrile (SAN) copolymerization system for certain copolymer compositions.

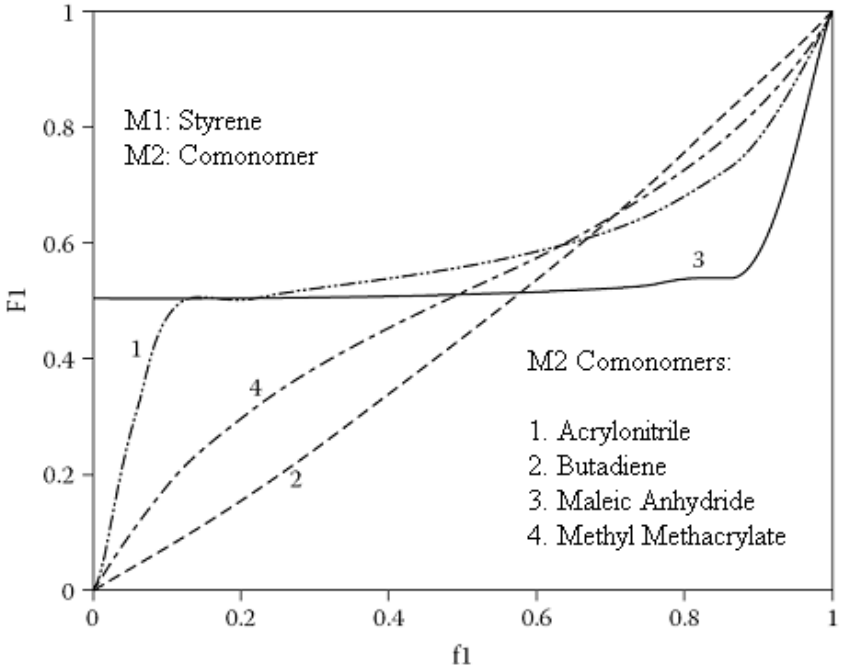

Figure 2.2 : Copolymer composition curves

2.3.2 Emulsion process of poly(styrene-*co*-acrylonitrile) (SAN) copolymers

Both batch (or semicontinuous) and continuous emulsion process are used to manufacture SAN latex [29]. In a batch process, a styrene, acrylonitrile, and aqueous solution of a water-soluble initiator, e.g., potassium persulfate), emulsifier, and chain transfer agent (molecular-weight regulator, e.g., dodecyl mercaptan) are charged into a stirred tank reactor. The weight ratio of styrene/acrylonitrile is generally kept between 70:30 and 85:15. If the desired copolymer composition corresponds to the azeotropic composition, copolymer composition drift will be minimal. Otherwise, a monomer mixture having a different styrene/acrylonitrile ratio from the initial charge must be added continuously during polymerization to keep the ratio constant because any wall deviation in the bulk monomer phase composition can easily result in significant composition heterogeneity. For example, two SAN copolymers differing more than 4% in acrylonitrile content are incompatible, resulting in poor physical and mechanical properties. To calculate the monomer feeding policy, a dynamic optimization technique can be used with a detailed process model. In such a process, the reactor temperature can also be varied to minimize the batch reaction time while maintaining the copolymer composition and molecular weight and/or molecular-weight distribution at their target values.

In a continuous emulsion process, two or more stirred tank reactors in series are used. Separate feed streams are continuously added into each reactor. The reactors are operated at about 68^{o}C. The latex is transferred to a holding tank (residence time of about 4 h) before being steam-stripped to remove unreacted monomers. In a continuous process, the residence time distribution is generally broad. A large holding tank placed downstream of the reactors provides extra time to the reaction mixture and reduces the molecular-weight distribution.

Mino [30] studied the bead copolymerization of styrene and acrylonitrile, in the presence of 1-azobis-1-phenylethane at high temperature (90-100°C) and determined the distribution of acrylonitrile between styrene and the aqueous phase in the conversion. The initial distribution of acrylonitrile between styrene and the aqueous phase and the change of this distribution during the copolymerization were determined. The concentration of acrylonitrile in the aqueous phase remains fairly constant up to 20-25% conversion, then it decreases rapidly up to about 90%

conversion. The over-all rate of copolymerization following an induction period, remains constant up to about 30-35% conversion, then it increases slightly only to decrease rapidly at about 90% conversion. In a system of this type the mole fraction of acrylonitrile in the oil phase increases through the polymerization, partly because acrylonitrile reacts at a lower relative rate, partly because the acrylonitrile dissolved in the aqueous phase diffuses continuously into the beads. The reactivities of styrene and acrylonitrile in aqueous dispersion are the same as in bulk if the partition of acrylonitrile between the two phases is taken into account. The initial rates of copolymerization, in bulk, increase with the acrylonitrile content of the mixture. At high conversion, a marked acceleration in rates takes place. This autoacceleration is due to the increased viscosity of the medium and to the variation of the comonomer composition with converting.

Beside the acrylonitrile dispersion, the initiator is important in emulsion polymerization of styrene-acrylonitrile copolymer. Medizabal et al. studied [31] the synthesis of styrene-acrylonitrile (SAN) copolymers by emulsion or microemulsion polymerization using either a water-soluble (potassium persulfate or KPS) or a water-insoluble (AIBN) initiator. The surfactant used was dodecyltrimethylammonium bromide (DTAB) or sodium dodecylbenzenesulfonate (SDBS). Polymerization in DTAB microemulsions initiated with AIBN are faster and have higher conversions than those initiated with KPS, but the opposite effect is observed for emulsion polymerization. In both emulsion and microemulsion polymerizations, high molecular weights (2-4 $\times 10^6$ Dalton) SAN copolymers are produced with composition richer in styrene (S/AN = 81/19 w/w) than the initial feed composition (75/25 w/w). Latex produced by microemulsion polymerization contain particles two- to three-fold smaller than those prepared by emulsion polymerization.

SAN copolymers are often manufactured at the azeotropic point, where monomer and polymer have the same composition [26, 29]. Vanderhoff et al. studied [32] Emulsion copolymerization of azeotropic styrene-acrylonitrile monomer mixture in polystyrene seed latexes. The azeotropic 80:20 styrene-acrylonitrile mixture was polymerized in 190nm and 300nm-diameter monodisperse polystyrene seed latexes by batch, batch-with-equilibrium-swelling, and semi-continuous polymerization. Polystyrene seed latexes were used to determine the degree of grafting of the substrate as well as the styrene-acrylonitrile copolymer. The critical factor

determining the formation of new particles was the surface area of the seed latex: at or above 226 m^2/dl, new particles were not formed; at or below 179 m^2/dl, a new crop of particles was nucleated, the number increasing with decreasing surface area. The degree of grafting of the polystyrene seed substrate was greater for the smaller particle size seed latex, and increased exponentially with increasing seed surface area. The amount of grafted styrene-acrylonitrile copolymer determined the stability of the grafted particles in acetone, a good solvent for the copolymer. Dynamic mechanical spectroscopy showed that the continuous phase was either the polystyrene substrate (T_g 104°C) or the styrene-acrylonitrile copolymer phase (T_g 120°C) except where the degree of grafting was high, in which case, the T_g was intermediate between the two values. Beside this study, Lin et al. studied [33] simulation model for the emulsion copolymerization of acrylonitrile and styrene in azeotropic composition. A simulation model based on the "unit segment" concept which provides prediction of conversion and molecular weight of product, is proposed for the emulsion polymerization of acrylonitrile and styrene in azeotropic composition. Effects of initiator concentration and emulsifier concentration on conversion and molecular weight were studied experimentally and theoretically. It is found that the desorption of acrylonitrile radicals should be taken into account, and the number of radicals per particle is always less than 0,5. The concentration of polymer particles is proportional to the 0.58 power in respect of the emulsifier concentration and to the 0,35 power in respect of the initiator concentration. The auto-acceleration effect becomes significant when both initial emulsifier concentration and initiator concentration decrease, which influences the average molecular weight of the products. The azeotropic composition of acrylonitrile/styrene is 28,5:71,5 by weight for this system at 60°C reaction temperature.

2.3.3 Suspension process of poly(styrene-*co*-acrylonitrile) (SAN) copolymers

Suspension polymerization is performed by using a single reactor or two paralel reactors [34]. A mixture of monomers, monomer-soluble initiator (peroxides and azo compounds), and any additives (e.g. chain transfer agents) is dispersed in water by mechanical agitation in the presence of a suspension stabilizer. The suspension polymerization temperatures range from 70°C to 125°C. The reactor temperature is

increased gradually during the batch. SAN copolymer particles of 10–3000 μm are obtained. To keep the copolymer composition constant, a mixture of monomers is added into the reactor as in emulsion processes.

Kido et al. reported the suspension copolymerization of acrylonitrile-styrene [35]? using dilauroyl peroxide and the $SnCl_2$ redox system. In suspension copolymerization of acrylonitrile-styrene, mixtures of 10–40 wt% acrylonitrile and 40–90 wt% styrene are polymerized in H_2O in the presence of inorganic dispersing agents according to the typical recipe presented in Table 2.3, to produce transparent copolymer beads containing >90% 100–400-μ mesh particles.

Table 2.3: Typical recipe: Suspension copolymerization of acrylonitrile and styrene*

Ingredients	**Amount (ppm)**
Water	150
Hydroxylapatite	2
Polyethylene glycol alkyl aryl ether phosphate	0,01
$SnCl_2$ x $2H_2O$	0,02
Acrylonitrile	25
Styrene	75
tert-Dodecyl mercaptan	0,5
Dilauroyl peroxide	0,71
HCCl– CCl_2	240

*Polymerization for 1 h at 25°C followed by 15 h at 60°C at stirring rate of 400 rpm.

Also, the acrylonitrile–styrene copolymer [36] was prepared by suspension polymerization in the presence of 0,005–0,05% (based on monomers) *tert*-Bu, 3,5,5-trimethyl perhexanoate, and *tert*-butyl peracetate at 110–140°C according to a typical recipe presented in Table 2.4 to give a copolymer (unreacted monomer 0,1%) with lower yellow neon and haze than a control (unreacted monomer) prepared without *tert*-Bu peracetate.

Table 2.4: Typical recipe: suspension copolymerization of styrene and acrylonitrile*

Ingredients	Amount (g)
Water	25.000
$Ca_3(PO_4)_2$	150
Styrene	11.000
Actylonitrile	6.000
tert-Butyl 3,5,5-trimethyl perhexanoate	25
tert-Butyl peracetate	15
tert-$C_{12}H_{25}SH$	50

*Polymerization for 5 h at 100°C and 2 h at 125°C

2.3.4 Mass process of poly(styrene-*co*-acrylonitrile) (SAN) copolymers

The mass process has some advantages over emulsion and suspension processes in that it is free of emulsifiers and suspending agents and thus produces SAN copolymers having higher clarity and good color retention [37]. As no solvent is used, the viscosity of the reacting mass increases with conversion, and the removal of polymerization heat becomes a problem when the conversion of monomers exceeds ≤ 60–70%. The mass polymerization is performed in a jacketed reactor equipped with a reflux condenser at a temperature ranging from 110°C to 210°C. In a continuous process, 50–65% conversion obtained in a single reactor is further increased to 65–90% in the second reactor, which is typically a horizontal linear flow reactor. To handle the highly viscous reaction mass, the reaction temperature in the linear flow reactor is increased along the direction of flow. Mass polymerization can be initiated either thermally or chemically by organic initiators. The polymer product is fed to a film evaporator, where unreacted monomers are recovered.

Arsac et al. studied [38] the mass free radical polymerization of SAN by thermal initiation and studied the rheological characteristics of SAN copolymers in compositions for different monomer feed ratios. Radical initiated polymerization of styrene with acrylonitrile was performed in the presence of 2,2'-azobisisobutyronitrile (2%) at 70°C with agitation. The polymeric products were purified after dissolving, precipitated in chloroform/methanol (volume ratio 1:8), and dried in vacuum at 80°C.

Beside free radical polymerization, mass polymerization can be applied via atom transfer radical polymerization. Al-Harthi et al. studied [39] atom transfer radical polymerization of styrene and acrylonitrile via mass polymerization with monofunctional and bifunctional initiators. A bifunctional initiator (benzal bromide) was used to initiate the bulk atom transfer radical polymerization of styrene and acrylonitrile at 90^{o}C with CuBr/2,2-bipyridyl. Bulk atom transfer radical polymerization of styrene and acrylonitrile with a bifunctional (benzal bromide) and monofunctional initiator (1-bromoethyl benzene) was successfully conducted in this investigation.

2.4 Polymer-Clay Nanocomposites

Within the fascinating world of nanomaterials in general, polymer–clay nanocomposites carry on their weight in terms of intrigue and applicability [40]. Consider all the factors that must be involved in the dramatic modification and improvement of a polymer's behavior upon the addition of just a few weight percent (wt%) of a nano-size inorganic sheet compound. Tensile modulus and strength can be doubled and the heat distortion temperature dramatically increased (by 100°C), without any sacrifice in impact resistance, upon the addition of just 2% by volume of this compound to nylon, for example. These inorganic, layered silicate species are clays. It is so-called smectite clays that are exploited in polymer–clay nanocomposite (PCN) synthesis. Smectites are a class of layered clays that are swellable in water and contain a significant cation exchange capacity at about 80 meq/100 g (this means that there are 80 meq of exchangeable cation per 100 g of clay). The fundamental inorganic unit is comprised of two tetrahedral silicate layers that sandwich a central metal octahedral layer (Figure 2.3).

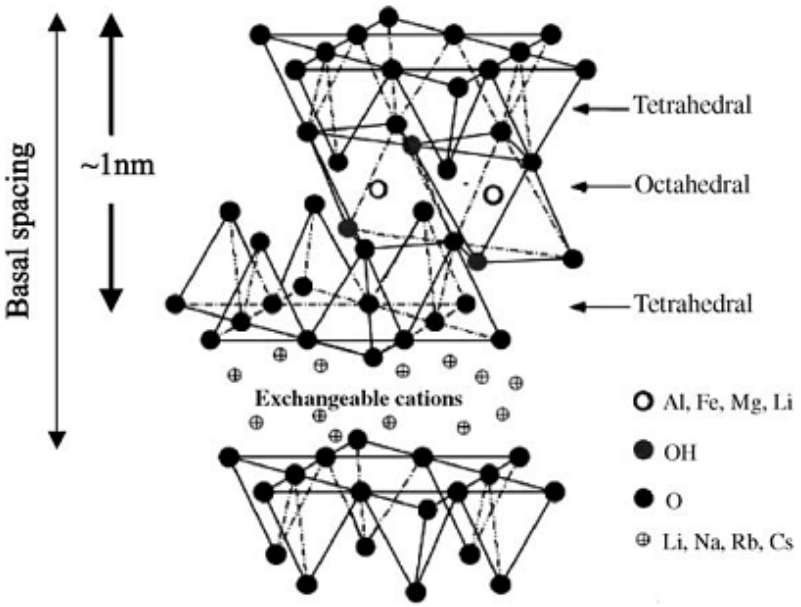

Figure 2.3 : Schematic representation of a montmorillonite smectite clay stucture

Idealized formulas for montmorillonite, the aluminum-based version, and hectorite, the magnesium-based version, are $Ex_{0.66}[Si_8Al_{3.34}Mg_{0.66}O_{20}(OH)_4]\cdot H_2O$ and $Ex_{0.66}[Si_8Mg_{5.34}Li_{0.66}O_{20}(OH,F)_4]\cdot H_2O$, respectively. Notice the isomorphous substitution of these clays, primarily within the octahedral layer, which gives rise to a net negative charge on the basal oxygen surfaces. This is compensated for by the presence of hydrated exchangeable cations in the interlayer or gallery regions, which in nature are usually alkali or alkaline earth cations. These cations are easily exchanged by larger species such as long-chain alkylammonium ions. The distance from one basal surface to the next in registry is called the basal spacing and is measured as the lowest angle peak in x-ray powder diffraction spectra. Natural clays have basal spacings in the range of 1,2 to 2,0 nm, depending on the type of cation and the amount of water present. This ability to swell is one of the most important characteristics of a smectite clay. They can, in fact, swell so greatly in some situations, such as in the presence of large concentrations of macromolecules, that the sheets can lose interaction with each other, the registry is lost, no basal spacing is observed, and the system is said to be exfoliated.

Other clays have been exploited in PCN research as well, including saponite, beidellite, and a synthetic swelling fluorine–mica. All are smectites, with differences primarily in elemental composition, cation exchange capacity, abundance, aspect

ratio, and particle size. The interactions of smectite clays with polymeric molecules both in nature and for industrial applications have been exploited for quite some time, although the development of polymeric nanocomposites has occurred fairly recently.

2.4.1 Polymer-clay nanocomposite architectures

There are two end members that describe the realm of structures possible in polymer–clay nanocomposites [41]. At one end of the spectrum are well-ordered, stacked multilayers that result from intercalated polymer chains within host silicate clay layers. At the other end of the spectrum are exfoliated materials, wherein the host clay layers have lost their entire registry and are well dispersed within a continuous polymer matrix. These two cases are shown schematically in Figures 2.4a and b.

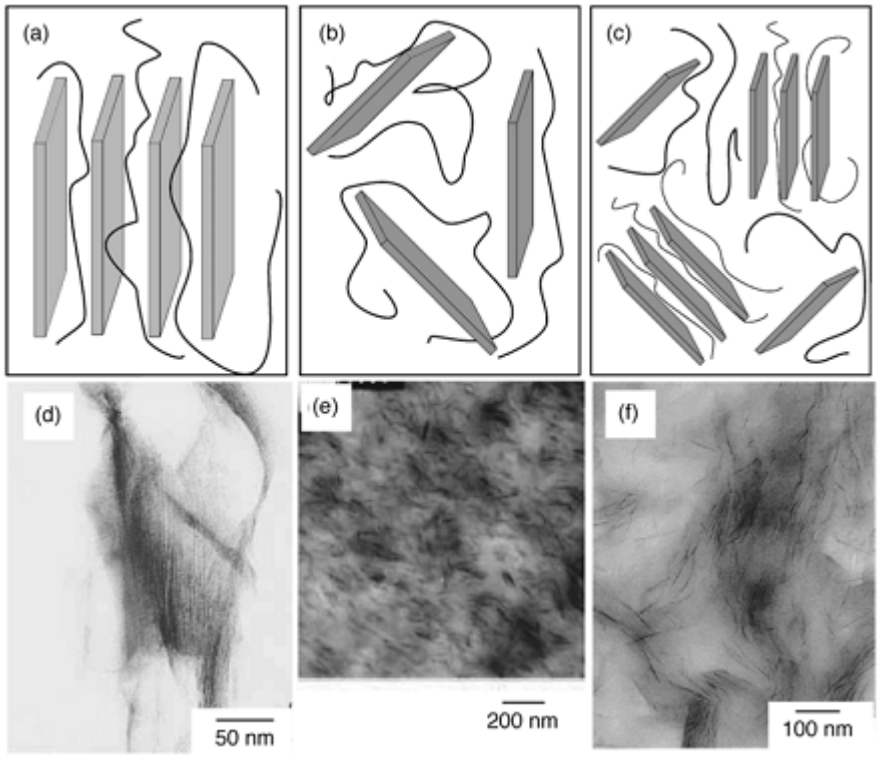

Figure 2.4 : Schematic representation of the various PCN architectures: (a) intercalated, (b) exfoliated, and (c) mixed intercalated–exfoliated. TEM images of actual PCN hybrids assigned to these various structures: (d) intercalated polystyrene–fluorohectorite showing 2,9-nm registry, (e) exfoliated nylon montmorillonite, and (f) a mixed intercalated exfoliated epoxy–montmorillonite (10% clay).

Exfoliated (also called delaminated) polymer–clay nanocomposites display acceptable stiffness, strength, and barrier properties with far lower ceramic content than is achieved for more conventional particulate-filled (e.g., glass fibers) polymer composites. Generally, the larger the degree of exfoliation in polymer–clay nanocomposites, the greater the enhancement of these properties. Figure 2.4c provides an idealized view of a mixed intercalated–exfoliated structure. All three of these morphologies have been observed, and representative transmission electron microscopy (TEM) images of each are provided in Figures 2.4d, e and f as well.

Often, there are occasions where retention of the layered nature of a polymer-clay nanocomposite is the desired outcome. Such regular nanoassemblies have the following unique characteristics and applications:

- There are a wide variety of both host materials (clay and nonclay) and polymers.
- Anisotropic arrangements of polymers in two-dimensional microenvironments occur.
- The variable gallery spacing is adaptable to polymer size.
- Microenvironments can induce spatial chemistry and host surface chemistry effects.
- Rigid host layers provide enhancements to structural, chemical, and thermal stabilities to more fragile guest polymers.

Two primary methods are utilized to prepare intercalated polymer–clay materials. These are shown schematically in Figure 2.5 as direct intercalation and as in situ polymerization of preintercalated monomers.

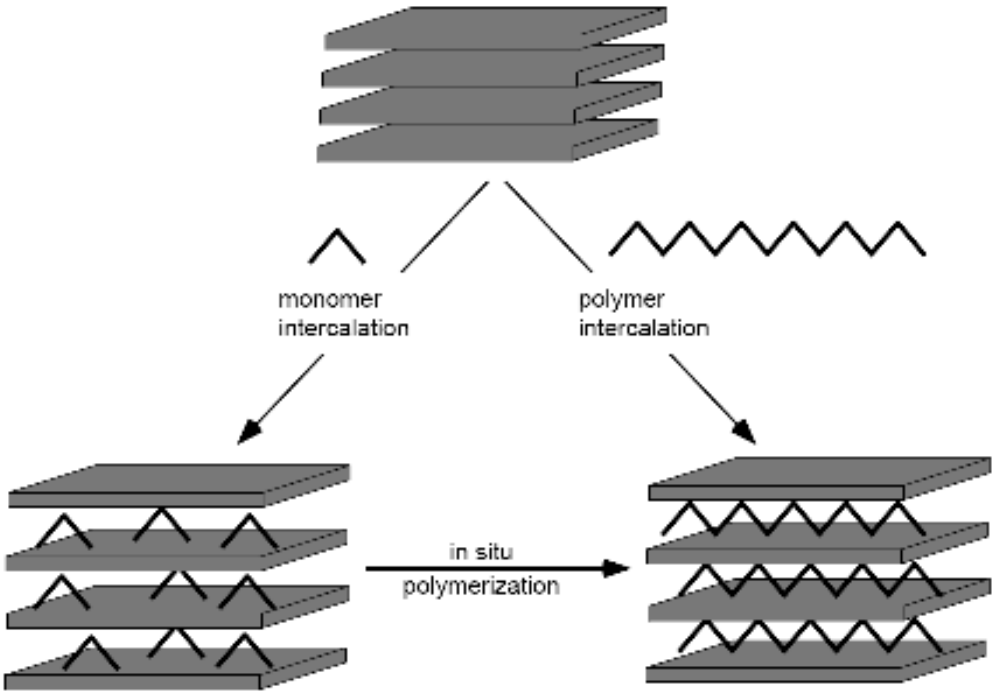

Figure 2.5 : Methods for creating intercalated polymer–clay architectures via direct polymer contact (usually in solution) and via *in situ* polymerization of preintercalated monomers.

Another way to intercalate polymers directly is through a melt method, where the polymers are heated with a preexfoliated (in most cases) clay. In this way, a conventional polymer extrusion process can often be utilized. The formation of PCNs via melt intercalation depends on the thermodynamic interaction between polymer chains and host layers, and also on the diffusion of polymer chains from bulk to interlayers.

The most successful process for making exfoliated PCNs has been through the polymerization of monomers that are in the presence of clay minerals. Conditions must be optimized to promote a polymerization that causes the uniform dispersion of silicate layers within the polymer matrix. The heat of reaction evolved (enthalpy) during polymerization provides an essential component to the exfoliation. Therefore, exfoliation is enhanced with increasing amounts of intercalated monomers and with decreasing layer charge on the clay surface.

Mixed intercalated–exfoliated systems in many cases contain units of just a few intercalated clay layers, rather than an entire extended registry, that are themselves

randomly oriented within the polymeric matrix. In most of these cases, conditions can be varied to foster full exfoliation.

2.4.2 Poly(styrene-*co*-acrylonitrile)–montmorillonite (SAN-Mt) composites

Interest in hybridizing clays into polymers at the nanoscale level is intense due to the pronounced improvements in properties at surprisingly low clay contents [42]. Examples of improvement are the increases in mechanical strength, modulus, thermal stability, gas barrier properties, fire-retardant properties, corrosion resistance, ionic conductivity and decreased absorption in organic liquids. The low dielectric constant of polymers leads to applications as electronic insulating materials. However, the dielectric response of polymer–clay nanocomposites are seldom studied.

Various nanocomposites have been synthesized by different methods in the development of reinforcement materials. Dispersion of smectite clays and other layered inorganic materials that can be broken down into nanoscale building blocks within the polymer matrix has been recognized as an excellent method for the preparation of organic–inorganic nanocomposites. Layered smectite-type montmorillonite (Mt), a hydrous alumina silicate mineral whose lamellae are constructed from octahedral alumina sheets sandwiched between two tetrahedral silicate sheets, exhibits a net negative charge on the lamellar surface, which adsorbs cations such as K^+, Na^+, Ca^{+2} and Mg^{+2}. Compatibility with various polymers is accomplished by modifying the silicates with alkylammonium cations via a cation exchange reaction or with a silane-coupling agent via a grafting process. When Na^+ in the clay is exchanged with the intercalating agent, the clay possesses an excellent swelling rate in water, and its interlayer spacing becomes large enough for monomer penetration.

Exfoliated, intercalated or mixed intercalated-exfoliated SAN-Mt nanocomposites were synthesized by melt process or in situ process. Properties and morphology of SAN nanocomposites were investigated by Stretz et al [43]. They synthesized SAN nanocomposites by melt process. Interactions between SAN and a single organoclay were probed by varying the SAN copolymer composition. Sample preparation was accomplished by melt processing on a microcompounder followed by injection molding. The effect of the acrylonitrile content of SAN on the morphology and

properties of nanocomposites formed by melt mixing SAN with a single montmorillonite organoclay has been examined by several techniques. Digital analysis of TEM photomicrographs indicate that there may be a slight maximum in particle aspect ratio for composites with about 38 wt% acrylonitrile, and that the PS-based composite demonstrates significantly higher particle thicknesses and lower specific particle densities, indicating a poorly exfoliated system compared to the other SAN-based composites. Modulus enhancement, measured as the slope of the normalized modulus versus Mt content, was shown to increase with increasing acrylonitrile content. Increased acrylonitrile content in the copolymer led to measurable increases in melt viscosity and, therefore, increased the shear stress on the particles during mixing.

Beside the mechanical properties, thermal properties of SAN nanocomposites were investigated. Jang et al. [44] studied the effect of clay on the thermal stability of SAN copolymer. The mass ratio of styrene/acrylonitrile in SAN sample was 75/25 and the butadiene rubber content in ABS is 17 wt%. SAN and ABS polymers were melt-blended with montmorillonite type clay. Thermal behaviour of nanocomposites according to the TGA results demonstrated that as the rubber content in SAN increases, the thermal stability increased, and the incorporation of clay in SAN or ABS further increased the thermal stability.

Dispersion of the montmorillonite clay on the molecular scale in polymer matrices, thus producing nanocomposites, renders possible polymers with superior mechanical properties and thermal stability [45]. The interaction of the montmorillonite clay with polymers might give exfoliated, intercalated or immiscible polymer hybrid systems. Several techniques have been suggested to obtain such high performance polymers beside melt process. In situ intercalative polymerization proved to be a successful way also to obtain nanocomposites in which the montmorillonite clay was organophilized with some organic surfactant to impart miscibility. Khalil et al. [45]studied the bulk copolymerization of styrene–acrylonitrile monomers using styrene-N^+–montmorillonite complex as a comonomer in the polymerization. Using styrene-N^+–montmorillonite complex as a comonomer in the copolymerization of styrene–acrylonitrile is an effective method of achieving compatibility between montmorillonite clay and polymers and hence a strong bonding between the mineral and polymer matrix. FTIR analysis revealed the existence of the montmorillonite-

clay complex in the extracted polymer by the presence of the Si–O stretching vibration as a sharp peak at 1075 cm^{-1} but no peaks were observed by XRD in the extracted polymer sample. This might be due to the presence of a very small amount of exfoliated clay layers that are strongly miscible and adhere to the polymer sample.

In situ process may be applied by various polymerization methods. SAN-Mt nanocomposites prepared by emulsion and solution polymerization were compared by Noh et al [46]. Nonextractable styrene–acrylonitrile copolymer–montmorillonite (SAN–Mt) nanocomposites were prepared by two different intercalation process: (1) a usual one-step emulsion copolymerization in the presence of the Na^{+}–Mt; and (2) a solution copolymerization with Mt modified by dimethyl dihydrogenated tallow ammonium. The copolymerization conditions were set up to be the same. Many physicochemical properties, such as polymer loading into the interlayer of Mt, molecular masses of intercalated polymer, gallery expansion, thermal stability, mechanical properties, and dispersibility of Mt in the polymer matrix of the emulsion product are found experimentally to far exceed those of products derived from the solution polymerization. This indicates that the use of emulsion polymerization is proven to be of great importance in preparing substantial polymer-clay hybrid nanocomposite.

3. EXPERIMENTAL PART

3.1 Materials

Clay	: The clay sample had the chemical composition (wt.%): SiO_2 70,30; Al_2O_3 15,00; Fe_2O_3 1,10; CaO 1,60; MgO 2,30; Na_2O 1,45; K_2O 1,20; TiO_2 0,30, ignition loss 6,45. Na-Montmorrilonite (CEC value: 135 meq) from Ordu, Ünye region purified, dried and modified with NaCl [47].
Sugar Beet Molasses	: Kastamonu Sugar Factory
Ceric Ammonium Nitrate	: (Merck) Dried in drying oven
(w/w) 65% HNO_3 Solution	: (Merck) Used in stock solutions
Styrene	: (Fluka) Kept in a fridge at -10^oC before use.
Acrylonitrile	: (Merck) Kept in a fridge at -10^oC before use.
Acetone	: (Commercial) Used for precipitation of polymers and nanocomposites.
DMF	: (Merck) Used as solvent in rheology analysis

3.1.1 Preparation of stock solutions

Stock solutions containing $(NH_4)_2Ce(NO_3)_6$ and HNO_3 were prepared with the same method. Desired amount of $(NH_4)_2Ce(NO_3)_6$ and 65% HNO_3 (w/w) solution were diluted to 100 ml with distilled water. Amounts of $(NH_4)_2Ce(NO_3)_6$ and 65% HNO_3 (w/w) solution used in stock solutions are given in Table 3.1.

Table 3.1: Amounts of $(NH_4)_2Ce(NO_3)_6$ and (w/w) 65% HNO_3 solution used in stock solutions

Stock solution	$(NH_4)_2Ce(NO_3)_6$ (g)	(w/w) 65% HNO_3 (ml)
0,1 N $(NH_4)_2Ce(NO_3)_6$; 0,1 N (w/w) 65% HNO_3	5,48	0,7
0,1 N $(NH_4)_2Ce(NO_3)_6$; 0,2 N (w/w) 65% HNO_3	5,48	1,4
0,1 N $(NH_4)_2Ce(NO_3)_6$; 0,33 N (w/w) 65% HNO_3	5,48	2,3
0,1 N $(NH_4)_2Ce(NO_3)_6$; 0,5 N (w/w) 65% HNO_3	5,48	3,4
0,1 N $(NH_4)_2Ce(NO_3)_6$; 1 N (w/w) 65% HNO_3	5,48	6,9
0,33 N $(NH_4)_2Ce(NO_3)_6$; 0,2 N (w/w) 65% HNO_3	18,09	1,4
0,33 N $(NH_4)_2Ce(NO_3)_6$; 0,5 N (w/w) 65% HNO_3	18,09	3,4

3.2 Instruments

Mechanical stirrer : Heildolph RZR1 TypeAC 220V, 50Hz.

Magnetic stirrer : AGE 10.0164, VELP Scientifica srl.

Vacuum : Shel-Lab vacuum drying oven was used for vacuum drying

Freeze Drier : Alpha 1-4 LD plus freeze drier was used to dry sugar beet molasses

FT-IR : Infrared spectra were recorded on disks of %1 w/w samples/KBr mixtures by Perkin Elmer spectrum one.

^{1}H-NMR : ^{1}H-NMR spectra were recorded with Bruker 250 MHz NMR Spectrometer and performed in DMSO-d_6 medium.

XRD : X-ray diffraction measurements were performed on Pan Analytical X-pert Pro model X-ray diffractometer at room temperature using Ni-filtered Cu-K_α radiation between $2\theta=2^o$-10^o.

Viscometer : The flow behavior of dispersions was determined with Brookfield CAP 2000+ Viscometer. CAP Spindle: CAP-S-01

DSC	: DSC analysis were performed with TA Instruments Q10 and TA Instruments Q1000
TGA	: TGA analysis were performed with TA Instruments Q50
DMA	: DMA analysis were performed with TA Instruments Dynamic Mechanical Analyzer (DMA) Q800

3.3 Synthesis of Monosaccharide-Mediated Poly(styrene-*co*-acrylonitrile) (MSAN)

Synthesis of MSAN has been performed with different conditions to obtain maximum yield. Optimum conditions which lead to 82% yield are given below.

A 250 ml round-bottomed three necked flask was equipped with a magnetic stirrer, a reflux condenser and a thermometer. The system was plunged into oil bath of which temperature had been formerly set to 50^{o}C. The temperature of the system has been monitored by the thermometer. 2 g of molasses and 125 ml of distilled water were added to the flask and stirred with magnetic stirrer for 15 min. 17,5 ml of acrylonitrile and 6,5 ml of styrene were added to the reaction mixture and stirred for 15 min. 25 ml of 0,33N $(NH_4)_2Ce(NO_3)_6$/0,2 N HNO_3 stock solution was dropped into the flask with dropping funnel during 20 min. Reaction has continued for 1h. The product was filtered, washed with acetone and dried in vacuum.

3.4 Synthesis of Monosaccharide-Mediated Poly(styrene-*co*-acrylonitrile)-NaMt Nanocomposites (MSAN/NaMt)

(MSAN/NaMt) synthesis was performed by adding different amounts of clay to the reaction conditions explained in part 3.3.

0,11 g (%0,5), 0,22 g (%1), 0,33 g (1%) and 0,44 g (2%) of clay were placed to the 250 ml round-bottomed three necked flask. 2 g of molasses and 125 ml of distilled was added. Reaction mixture has been stirred with mechanical stirrer for 24 h at 50^{o}C. Then, 17,5 ml of acrylonitrile and 6,5 ml of styrene were added to the mixture and stirred for 15 min. 25 ml of 0,33N $(NH_4)_2Ce(NO_3)_6$/0,2 N HNO_3 stock solution was dropped with dropping funnel during 20 min. Reaction has continued for 1 h. The product was filtered, washed with acetone and dried in vacuum.

4. RESULTS AND DISCUSSION

The results obtained from this work will be investigated in three sections:

- Preparation of monosaccharide-mediated poly(styrene-*co*-acrylonitrile) copolymers (MSAN) by redox polymerization and their characterizations.
- Preparation of monosaccharide-mediated poly(styrene-*co*-acrylonitrile)-NaMt nanocomposites (MSAN/NaMt) by *in situ* polymerization and characterizations of nanocomposites obtained.
- Comparison of copolymers and composites obtained in terms of their rheologic, morphologic, thermal, mechanic and water absorption properties.

4.1 Synthesis and Characterization of MSAN

Styrene and acrylonitrile were expected to react in the presence of molasses to form MSAN copolymer.

Molasses is known to be formed of 46-48% sugars such as glucose, fructose, raffinose and unseperated sucrose etc [8]. It was used in the reactions as a source of monosaccharides and at the same time, utilization of molasses was aimed. Reaction is thought to proceed on radical polymerization in aqueous system using ceric ion/nitric acid redox initiator. Mechanism of ceric ion reaction is known to be based on formation of a chelate complex and it decomposes to generate free radical sites [48, 49].

Monosaccharides are the molecules which include alcohol groups. Free radicals are produced via oxidation of monosaccharides by Ce(IV). Monosaccharide molecule and Ce(IV) produce a complex and decompose to generate free radical [50]. The reaction mechanism which best explains the products and kinetics of glucose oxidation by Ce(IV) is depicted below (4.1).

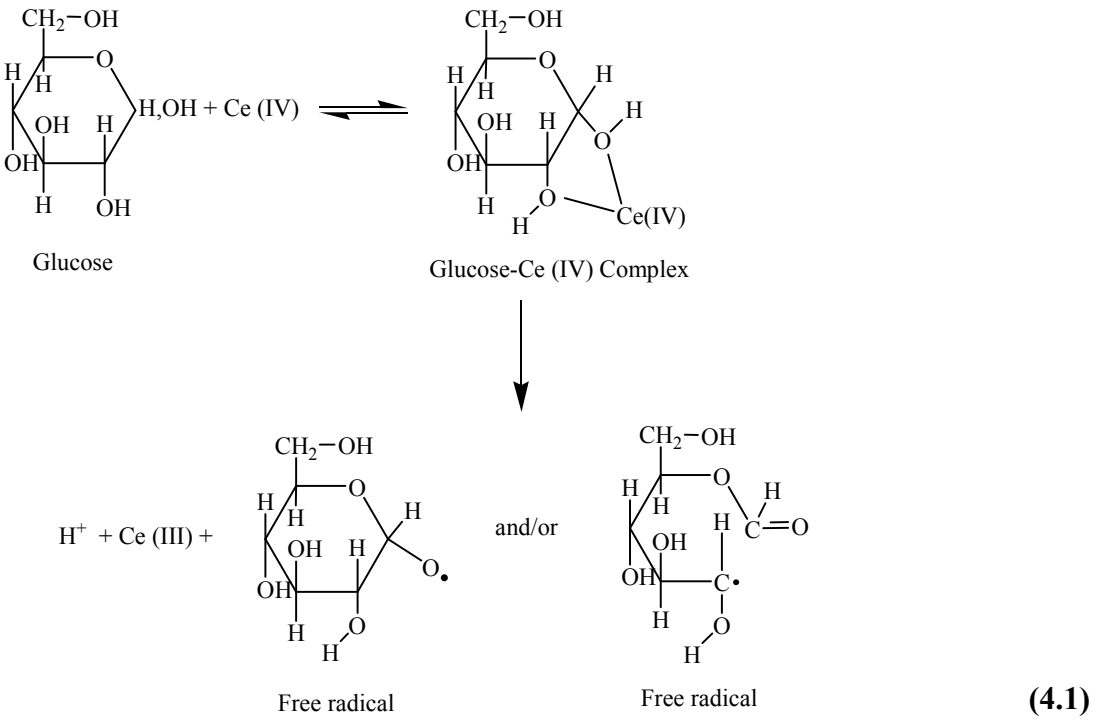

(4.1)

Molasses contain monosaccharides such as glucose, fructose, raffinose, unseperated sucrose etc [8]. It was expected monosaccharides in molasses to act as reducing agents to reduce Ce(IV) to Ce(III). The aim was the free radicals generated on monosaccharides to initiate polymerization. Possible reaction mechanism is given below (4.2).

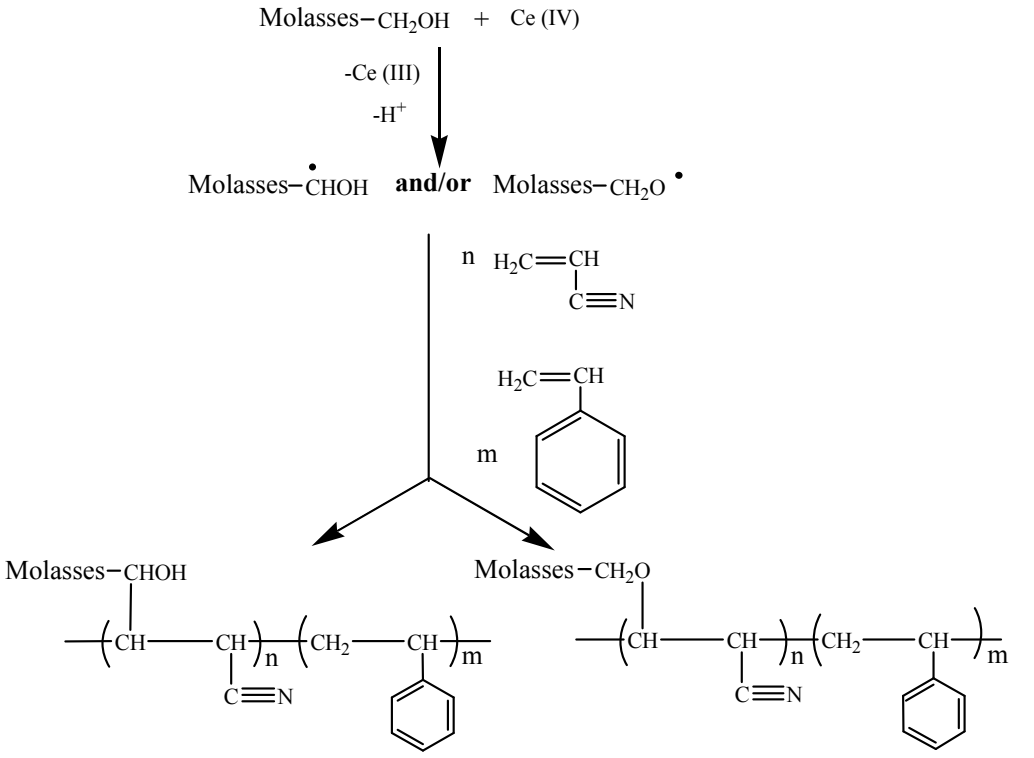

(4.2)

Reactions were performed at 50°C during 1h. It was seen that dropping time of Ce(IV)/HNO_3 solution does not have an appreciable effect on yield while concentrations of monomers, molasses, Ce(IV) and HNO_3 were effective on the yield of product. So that, reaction conditions of experiments were changed in terms of these parameters (Table 4.1).

Reaction conditions were changed in the parameters of molasses, acrylonitrile, styrene, Ce(IV) concentration and HNO_3 concentration. The path followed to obtain maximum yield and desired products, and the results were discussed according to the parameters below.

Molasses concentration

In the experiments of MSAN54-56-57, molasses concentration were kept at 4 g/L, 4g/L, 3g/L respectively. However, the yield of these experiments were low. So that, in other experiments, concentration of molasses were increased. In the experiments of MSAN68 and MSAN69, all of the conditions were kept the same except molasses concentration. These experiments indicates the optimum concentration as 12 g/L.

Ce(IV) concentration

In the experiments, Ce(IV) solutions in different concentrations were used. Concentration of Ce(IV) in reaction solution was an effective parameter on the yield. Reaction conditions of MSAN68 and MSAN71 were the same except Ce(IV) concentration. When they were compared, optimum Ce(IV) concentration was decided to be 48,53 mmol/L Ce(IV) solution

HNO_3 concentration

HNO_3 concentration was changed in the experiment while the other conditions were fixed. Experiments of MSAN60-63-64 have the same conditions except HNO_3 concentration. Likewise, MSAN59 have the same conditions with MSAN65 and MSAN67 except HNO_3 concentration. HNO_3 concentration was changed as 55 mmol/L, 166,7 mmol/L and 16,7 mmol/L in MSAN60-63-64. Comparison of MSAN60-63-64 shows the maximum yield (17%) obtained by using 55mmol/L HNO_3. However, in the experiments of MSAN59-65-67, HNO_3 concentrations were changed as 56,9 mmol/L, 86,2 mmol/L and 34,5 mmol/L respectively. Comparison of them shows that highest value of yield (21%) gets stable at about 56,9-34,5 mmol/L HNO_3. So, concentration of HNO_3 was prefered as 34,5 mmol/L.

Table 4.1: Reaction conditions of synthesis of MSAN during 1 h at 50°C

Experiment	Molasses	Acrylonitrile	Styrene	Ce(IV)	HNO_3	Yield
	(g/ L)	ml (mole/L)	ml (mole/L)	mmole/L	N (mmol/L)	%
MSAN54	4	5 (0,33)	5 (0,31)	14,04	0,5 (21,3)	22
MSAN56	4	5 (0,41)	5 (0,38)	17,07	0,5 (25,9)	0
MSAN57	3	10 (0,64)	5 (0,30)	13,56	0,5 (20,6)	8
MSAN59	14	15 (0,97)	5 (0,30)	17,24	0,33 (56,9)	21
MSAN60	13	15 (0,94)	10 (0,58)	16,67	0,33 (55)	17
MSAN63	13	15 (0,94)	10 (0,58)	16,67	1 (166,7)	0
MSAN64	13	15 (0,94)	10 (0,58)	16,67	0,1 (16,7)	11
MSAN65	14	15 (0,97)	5 (0,30)	17,24	0,5 (86,2)	5
MSAN66	12	10 (0,57)	5 (0,25)	15,15	0,2 (30,3)	24
MSAN67	14	15 (0,97)	5 (0,30)	17,24	0,2 (34,5)	21
MSAN68	12	15 (0,83)	5 (0,26)	14,71	0,2 (29,4)	25
MSAN69	24	15 (0,83)	5 (0,26)	14,71	0,2 (29,4)	16
MSAN71	12	15 (0,83)	5 (0,26)	48,53	0,2 (29,4)	46
MSAN74	12	7,5 (0,41)	15 (0,75)	47,8	0,2 (29)	32
MSAN78	12	17,5 (0,95)	6,5 (0,33)	47,4	0,2 (28,7)	82

Monomers

In the experiments, monomer amounts were changed to obtain maximum yield and to obtain the product in various monomer ratios in polymer chain. In experiments of MSAN59 and MSAN60, reaction conditions were almost the same except styrene concentration. In these experiments, it can be seen that yield has decreased when styrene concentration has been increased from 5 ml (0,3 mol/L)) to 10 ml (0,58 mol/L)) while acrylonitrile concentration was 15 ml (~0,97 mol/L). In the same way, experiments of MSAN66 and MSAN68 have almost the same reaction conditions except acrylonitrile concentration. In these reaction conditions, increasing acrylonitrile concentration from 10 ml (0,57 mol/L) to 15 ml (0,83 mol/L) caused the yield to increase from 24% to 25%. Considering these four reactions, MSAN71-74-78 experiments were performed by changing monomer concentrations. Experiments of MSAN71-74-78 have the same reaction conditions except monomer concentration. In experiments of MSAN71 and MSAN78 monomer concentrations were different but monomer ratios (w/w) were ~70% acrylonitrile and ~30% styrene. In these reaction conditions, MSAN78 had a higher yield than MSAN71 where monomer amounts were 17,5 ml (0,95 mol/L) of acrylonitrile and 6,5 ml (0,33 mol/L) of styrene. In experiment MSAN74, reaction was performed by using monomer ratios (w/w) of 30% acrylonitrile and 70% styrene reversely in experiment MSAN78. Yield of MSAN74 was obtained as a lower value than MSAN78.

Structures of molasses and product of MSAN78 were identified using FT-IR spectra.

In Figure 4.1, FT-IR spectra of molasses and MSAN78 can be seen.

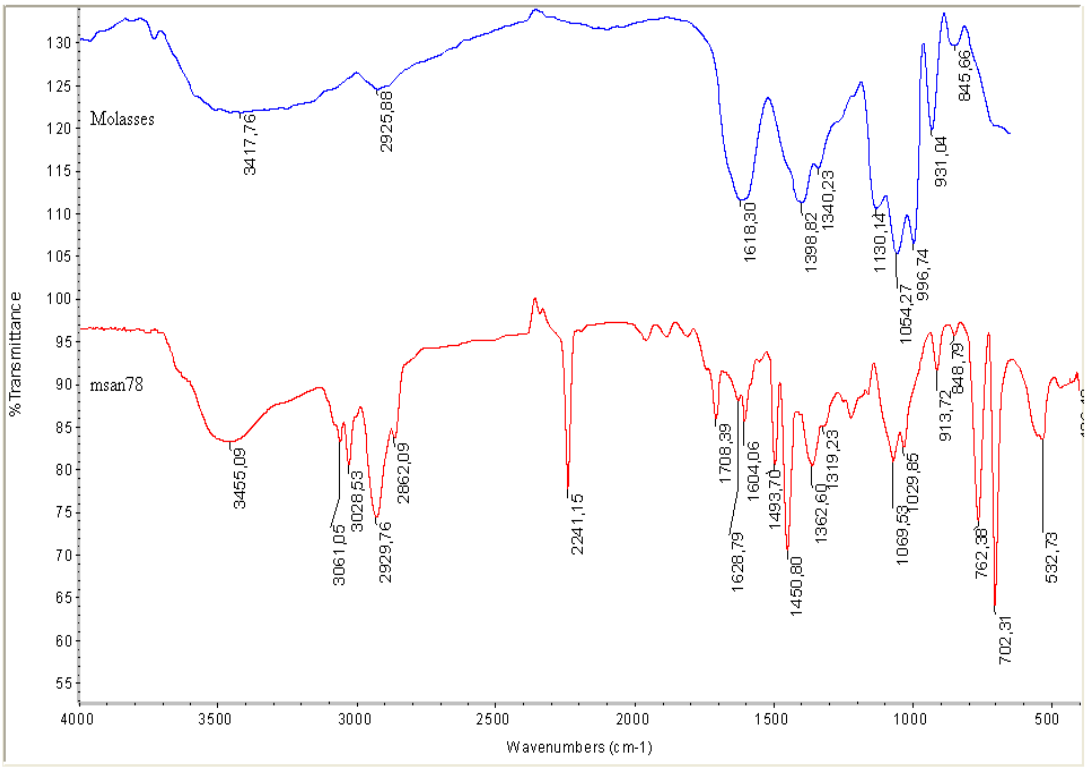

Figure 4.1 : FT-IR spectra of molasses and MSAN78

In FT-IR spectrum, absorption bands of molasses were determined as stretching vibrations of O-H bonds as a wide peak at 3455 cm^{-1}, aliphatic C-H bonds stretching vibrations at 2925 cm^{-1}, H-O-H deformation at 1618 cm^{-1} and, aliphatic C-H rocking vibrations at 1340 cm^{-1} and 1398 cm^{-1} (Figure 4.1). The peaks in the region of approximately 1000-1200 cm^{-1} (1130 cm^{-1}, 1054 cm^{-1}, 996 cm^{-1}) indicate C-OH and C-O-C bonds streching vibrations. The IR spectra of monosaccharides in the 1170-980 cm^{-1} region are sensitive to the axial and equatorial position of the C-OH groups which can affect quite significantly the main band positions. The characteristic anomeric region peaks are approximately 834 cm^{-1} for α-linkage and 898 cm^{-1} for β-linkage [51]. The peak at 845 cm^{-1} confirms the α-glycosidic bond vibrations and 931 cm^{-1} confirms the β-glycosidic bond vibrations. The characteristic peaks of molasses are the peaks at 845 cm^{-1} and 931 cm^{-1}.

In Figure 4.1 MSAN78 can be seen. In the spectrum, streching vibrations of O-H bonds were determined coming from molasses at 3455 cm-1. The peaks at 3061 cm^{-1} and 3028 cm^{-1} confirm stretching vibrations of aromatic C-H bonds belonging to styrene units in copolymer chain. Aliphatic C-H bond stretching vibrations of

copolymer chain are seen at the 2929 cm^{-1} and 2862 cm^{-1}. The sharp peak at 2241 cm^{-1} confirm the presence of C≡N bond belonging to the acrylonitrile units in copolymer chain. Aromatic C=C bond stretching vibration peaks are seen at 1628 cm^{-1} and 1604 cm^{-1}. The peaks at 1493 cm^{-1} and 1450 cm^{-1} are the peaks of aliphatic C-H bond bending and the peaks at 762 cm^{-1} and 702 cm^{-1} are the aromatic C-H bond rocking peaks. The band at 1708 cm^{-1} can be associated with carbonyl (C=O) stretching from a carboxylic acid. The presence of a carboxylic acid is possibly a result of the nitrile group hydrolysis in acid media [52].

The peaks belonging to aromatic C-H and C≡N streching vibrations confirm the copolymerization of styrene and acrylonitrile clearly.

Monosaccharides have small amounts in polymer chains. So, it is hard to see the characteristic peaks of molasses in MSAN78 FT-IR spectrum. For example, characteristic peaks of molasses at 845 cm^{-1} and 931 cm^{-1} may be overlayed with the peaks of styrene units at 913 cm-1 and 848 cm^{-1}. C-O-C bonds streching vibrations, belonging to molasses units, strengthens the peaks at 1029 cm^{-1} and 1069 cm^{-1}. Also, the peak at 3455 cm^{-1} which is the –OH streching vibrations confirms that molasses has reacted with copolymer chain.

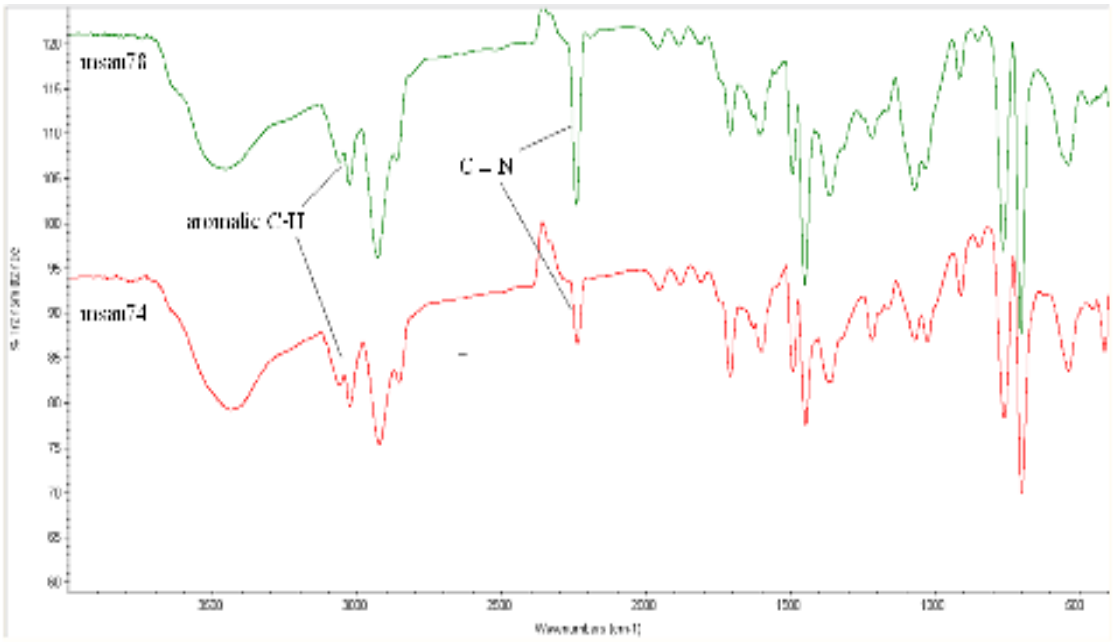

Figure 4.2 : FT-IR spectra of MSAN78 and MSAN74

The products obtained in experiments MSAN78 and MSAN74 were compared in Figure 4.2. Reaction conditions of these experiments were the same except monomer ratios. Monomer ratios in reaction solutions are %30 styrene; %70 acrylonitrile (w/w) in MSAN78 while it is %70 styrene; %30 acrylonitrile (w/w) in MSAN74. It is expected that mole fraction of monomers in copolymer chains to be varied due to the monomer ratios [26]. The product of MSAN74 is expected to have more number of styrene units than that of MSAN78. If FT-IR spectra of MSAN74 and MSAN78 are observed (Figure 4.2), it can be seen that C≡N stretching vibration peak of acrylonitrile units of MSAN78 is stronger than that of MSAN74, while aromatic C-H stretching vibration peaks of both product are nearly in the same strength. Considering this difference between two spectra, it is predicted that styrene mole fraction of MSAN74 copolymer chain is higher than that of MSAN78.

Structural identification of copolymers and molasses obtained by FT-IR were supported with ^{1}H-NMR analysis.

In Figure 4.3 and Figure 4.5, ^{1}H-NMR spectra of molasses and MSAN78 can be seen respectively.

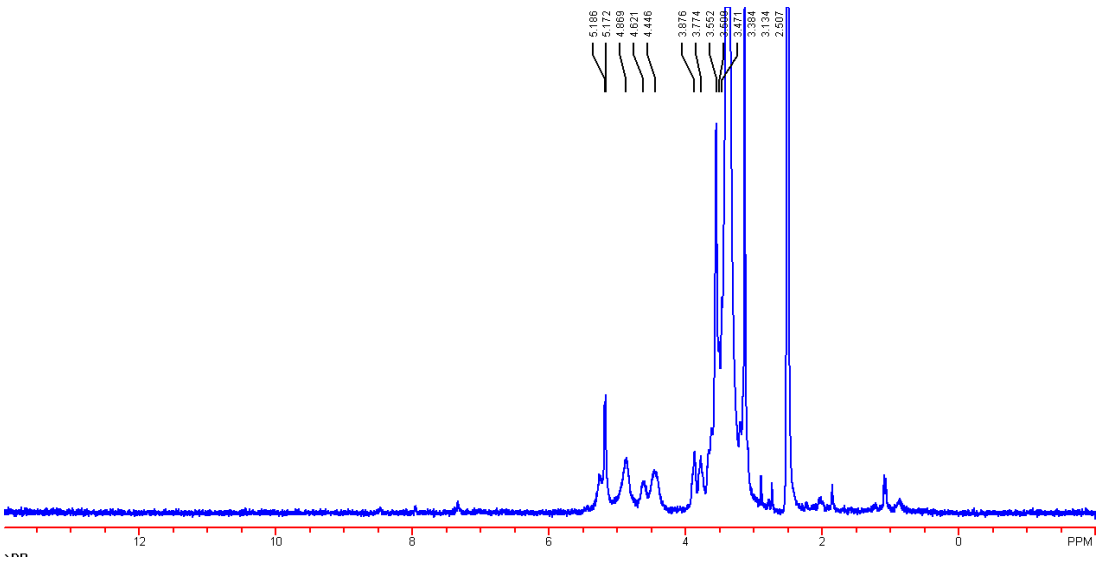

Figure 4.3 : ^{1}H-NMR spectrum of molasses

^{1}H-NMR spectrum of molasses is depicted in Figure 4.3. Characteristic peaks of molasses appear in the region between 3 ppm and 6 ppm. Molasses is known to be containing organic acids such as mainly lactic acid (1,7%), malic, fumaric, valeric, oxalic acids and the trace amount of glucuronic and galactronic acids where the total

organic acid content can reach up to 4% [7]. However, the amount of organic acids constitute a slight part of total molasses content (4%). So that, resonance of these organic acid protons cannot be observed in ^{1}H-NMR spectrum because of the predominant sugar content of molasses. Beside water, numerous non-sugar organic materials and the materials generated during the process and storing, constitute the composition of molasses [3]. The resonance of the protons of these materials may not be observed because of their slight amount or it may be difficult to distinguish their peaks from the predominant sugar resonance bands. It is predicted that the protons observed in ^{1}H-NMR spectrum, belong to the sugars due to high sugar content of molasses. The sugar content accepted for sugar beet molasses is 46-48% [7]. These sugars are mostly fermentable monosaccharides such as sucrose (remained), glucose, fructose and raffinose.

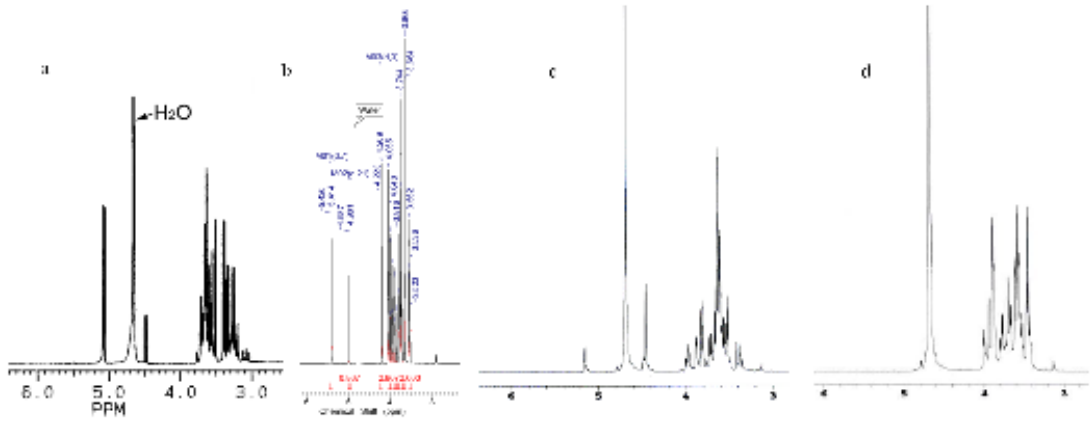

Figure 4.4 : ^{1}H-NMR spectra of glucose (a), raffinose (b), galactose (c) and fructose (d)

It is known that the resonance for protons of sugars generally appear between 3 ppm and 4 ppm [53, 54]. In Figure 4.4, ^{1}H-NMR spectra of glucose [54], raffinose [55], galactose and fructose [56] are depicted as example. In the ^{1}H-NMR spectrum of molasses, the signal at 3.38 ppm belongs to water (Figure 4.3). The signal at 5.1 ppm and 4.5 ppm shows the presence of the α and β anomeric protons of sugars, respectively [54]. The signals in the region between 3.4 ppm and 3.9 ppm, represent the resonance for protons of sugars in other positions.

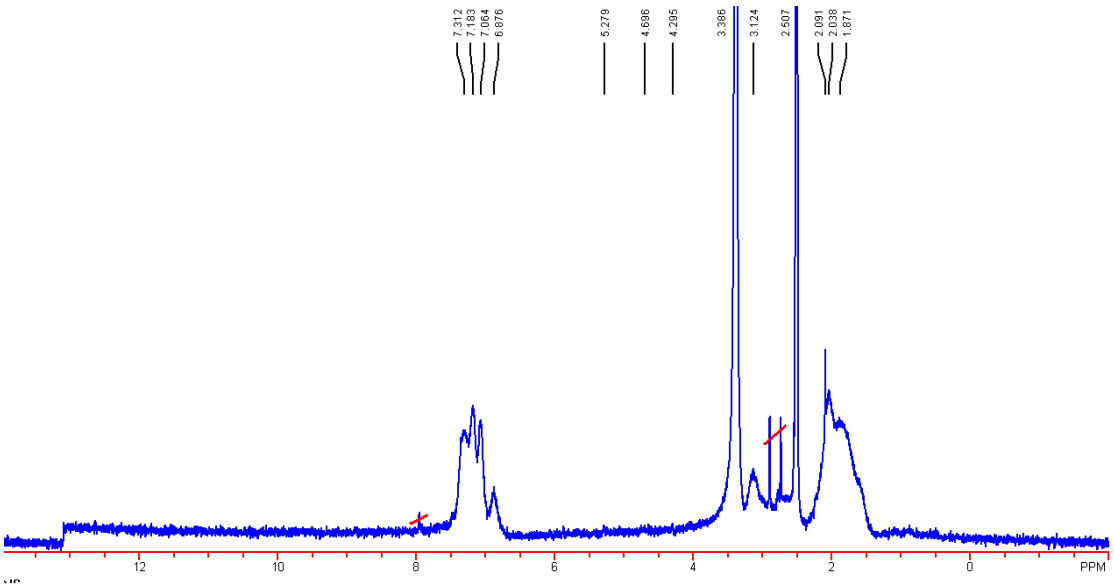

Figure 4.5 : ^{1}H-NMR spectrum MSAN78

The ^{1}H NMR spectrum of MSAN78 (Figure 4.5) shows broad peaks between 6.7–7.5 ppm (resonance of aromatic protons of styrene units) [57, 58]. Signal between 2.9–3.25 ppm, which shows peak maximum at 3.1 ppm, is the resonance of methine protons (-CHCN-) of acrylonitrile unit [59]. In ^{1}H-NMR spectrum of polyacrylonitrile homopolymer [59], resonance of methylene group (-CH_2-CH-) is observed as a broad peak between 1.7-2.4 ppm which shows peak maximum at 2.1 ppm. In ^{1}H-NMR spectrum of polystyrene homopolymer [58], resonance of methine (-CHC(C_6H_5)) and mehylene (-CH_2-CH-) groups appear as a broad peak between 1.1-2.4 ppm. In ^{1}H-NMR spectrum of MSAN78, resonance bands of methine group of styrene units and methylene groups of both of acrylonitrile and styrene units overlap and appear between 1.4-2.4 ppm. Sharp peak at 2.5 ppm is the signal of DMSO (solvent impurity) [59]. Sharp peaks with small intensities at 2.7 ppm, 2.9 ppm and 7.9 ppm come from DMF impurity in solvent (DMSO) [60, 61] (It is a fault a slight amount of DMF to be mixed into DMSO bottle). Peak at 3.38 ppm is most probably the resonance of water protons absorbed by DMSO, and also the resonance of molasses protons, with the water absorbed by it, overlap with this peak. However, amount of molasses content reacted with copolymer is very low so, it is expected them to seem as noise. Predictably, peaks belonging to molasses in the region of 4.2-5.4 ppm can be seen just as a noise in the spectrum of copolymer.

In Figure 4.6, comparison of ^{1}H-NMR spectra of molasses, MSAN78 and MSAN74 are shown.

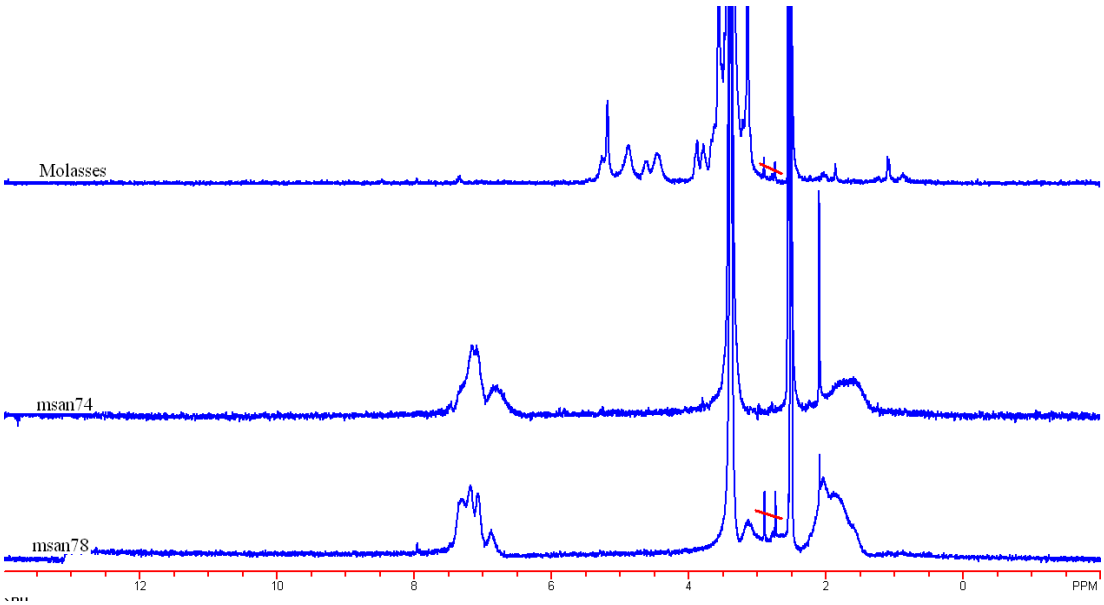

Figure 4.6 : ^{1}H-NMR spectra of molasses, MSAN74 and MSAN78

In spectra of MSAN78 and MSAN74, sharp peak at 2.5 ppm is the signal of DMSO (solvent impurity) [59]. Peak at 3.38 ppm is most probably the resonance of water protons absorbed by DMSO, and also the resonance of molasses protons, with the water absorbed by it, overlap with this peak. However, amount of molasses content reacted with copolymer is very low so, it is expected them to seem as noise. Predictably, peaks belonging to molasses in the region of 4.2-5.4 ppm can be seen just as a noise in the spectrum of copolymers. In spectra of MSAN78 and MSAN74 demonstrates that the signals of aromatic proton resonance (6.7–7.5 ppm) and the signals of methine group of styrene units and methylene groups resonance of both of acrylonitrile and styrene units (1.4-2.4 ppm) correspond each other. Both of the spectra prove the formation of SAN copolymer. However, in the spectrum of MSAN74, signals of methine group of styrene units appear discretely (2.1 ppm). Also, in spectrum of MSAN74 signals of methine group protons of acrylonitrile units cannot be observed clearly (3.1 ppm). These facts support the thougth of styrene units to have a higher percentage in MSAN74 copolymer chain than that of MSAN78 copolymer chain. Predictably, calculations of monomer fractions in polymer chains by the ratio of integral area of aliphatic group protons and aromatic group protons, demonstrate that copolymer MSAN78 consists of 40% styrene unit, 60%

acrylonitrile unit while copolymer MSAN74 consists of 55% styrene unit, 45% acrylonitrile unit When monomer ratios (w/w) and yields of experiments MSAN59-60-66-68-71-74-78 were compared, it can be seen that yield has been increasing while monomer ratio of acrylonitrile was converging to 70%. In the same way, yield decreases while styrene ratio was converging to 30%. In all of the experiment sets, yields were higher in experiments which had higher acrylonitrile ratio. As a result of experiments, MSAN78 was constituted as the experiment having optimum reaction conditions and (MSAN/NaMt) nanocomposites were prepared by performing reaction conditions of MSAN78.

4.2 Synthesis and Characterization of MSAN/NaMt

MSAN78 was the experiment having optimum reaction conditions. (MSAN/NaMt) samples were prepared by in situ polymerization performing reaction conditions of MSAN78. NaMt has been used in the experiments in various amounts as 0,5%, 1%, 1,5% and 2% (Table 4.2). Yield of the product obtained in MSAN78 was 82%. Yields of nanocomposites decreased to 58% and there was no change in yield while NaMt amount was increasing. Decrease in yield can be explained by interaction of copolymer and NaMt. Because of the interaction between molasses and NaMt, number of active centers on molasses decreases. Decrease in active centers causes a decrease in number of polymer chains.

Table 4.2: Amount of NaMt in (MSAN/NaMt) samples and yield of products

Experiment	NaMt		Yield
	g	% (w/w)	%
MSAN78	0	0	82
MSAN/NaMt80	0,11	0,5	58
MSAN/NaMt81	0,22	1	58
MSAN/NaMt82	0,33	1,5	58
MSAN/NaMt83	0,44	2	58

Structures and interactions between NaMt and copolymer were identified by FT-IR.

Structure of NaMt was explained and comparison of NaMt, MSAN78 and MSAN/NaMt80 obtained by using 0,5% NaMt were compared in Figure 4.7.

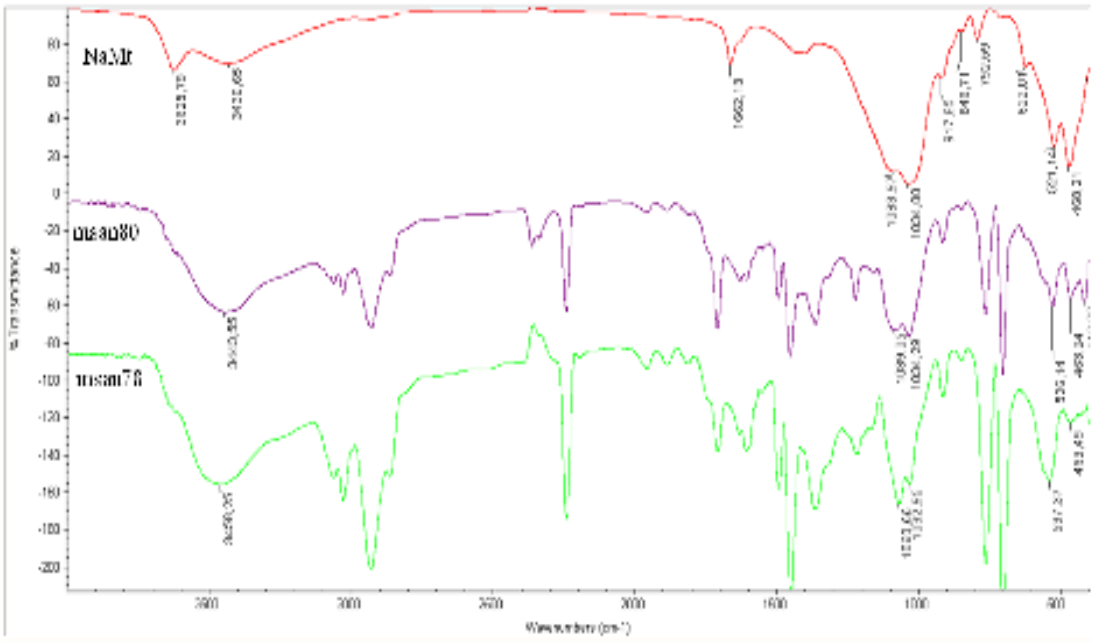

Figure 4.7 : FT-IR spectra of NaMt, MSAN78 and MSAN/NaMt80

Characteristic absorption bands of NaMt (Figure 4.7) were determined as structural (3625 cm^{-1}) and intra/intermolecular hydrogen bonded (3430 cm^{-1}) O–H stretching vibrations, H–O–H deformation vibration due to adsorbed water at 1662 cm^{-1}, Si–O stretching vibration at 1034 cm^{-1} with a shoulder at 1083 cm^{-1}, Al–OH (917 cm^{-1} and 622 cm^{-1}) and (Al, Mg)–O (846 cm^{-1} and 792 cm^{-1}) vibrations modes, Si–O bending vibration at 521 cm^{-1} and 468 cm^{-1}.

Comparison of MSAN78 and MSAN/NaMt80 demonstrates the same characteristic SAN bands (Figure 4.7). There is no significant difference between the signals of these copolymer samples except typical bands of NaMt in MSAN/NaMt80 spectrum.

In the spectrum of MSAN/NaMt80, structural O–H stretching of NaMt at 3625 cm^{-1} could not be determined as a separate band, only observed as a shoulder to H-bonded O-H groups. In MSAN/NaMt80 spectrum, maximum peak of O-H groups is seen at 3443 cm^{-1} between the molasses O-H bands (MSAN78) and NaMt hydrogen bonded O-H bands with a shift. Si-O stretching vibrations of NaMt are also seen at 1034 cm^{-1} and with a shift at 1089 cm^{-1}. Characteristic Si-O bending vibrations can be seen clearly in MSAN/NaMt80 spectrum while MSAN78 does not have these peaks. Si-O bending vibrations of NaMt at 521 cm^{-1} and 468 cm^{-1} has shifted to 526 cm^{-1} and 463 cm^{-1} and this is an evidence of interaction between NaMt and copolymer.

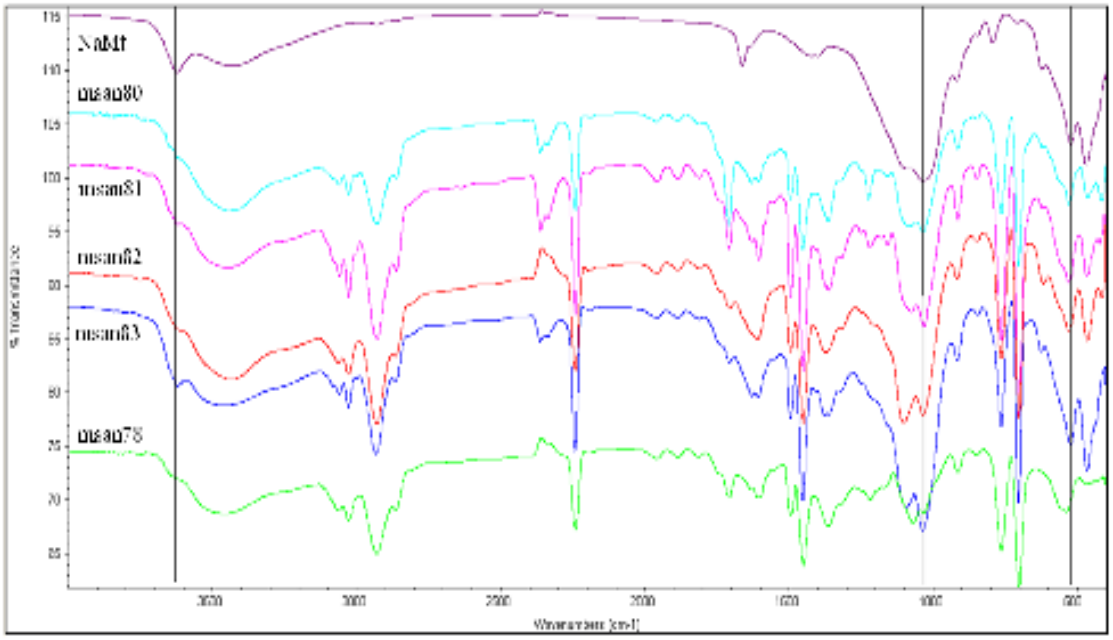

Figure 4.8 : FT-IR spectra of NaMt, MSAN78, MSAN/NaMt80, MSAN/NaMt81, MSAN/NaMt82 and MSAN/NaMt83

Comparison of FT-IR spectra of NaMt, MSAN/NaMt samples and MSAN78 can be seen in Figure 4.8. Structural O-H stretching vibrations of NaMt is determined at 3625 cm^{-1}. In composite samples (MSAN/NaMt80-81-82-83), it can be seen that both intensity and wavenumber (3622 cm^{-1}) of structural O-H band of NaMt decreased. This an evidence of interaction with structural O-H groups of NaMt with copolymer. By the increase in NaMt amount, Si-O stretching vibration bands shifted to greater wavenumbers (1034 cm^{-1} (NaMt), 1035 cm^{-1} (MSAN/NaMt80-81), 1038 cm^{-1} (MSAN/NaMt82), 1042 cm^{-1} (MSAN/NaMt83) and the strength of the bands increased. Si-O bending vibration bands of NaMt are at 521 cm^{-1} and 468 cm^{-1}. Si-O bending vibration bands at 521 cm^{-1} have an increase in both wavenumbers and intensity by addition of NaMt. Band of NaMt at 468 cm^{-1} has an increase in intensity by addition of NaMt but the wavenumbers of it shifted to smaller wavenumbers.

In Figure 4.9, ^{1}H-NMR spectra of MSAN78 and MSAN/NaMt80-81-82-83 are shown. All the signals in the spectra of copolymer and its nanocomposites correspond each other proving the formation of MSAN copolymer. Structures of nanocomposites are the same as MSAN78 due to their signals in the same regions.

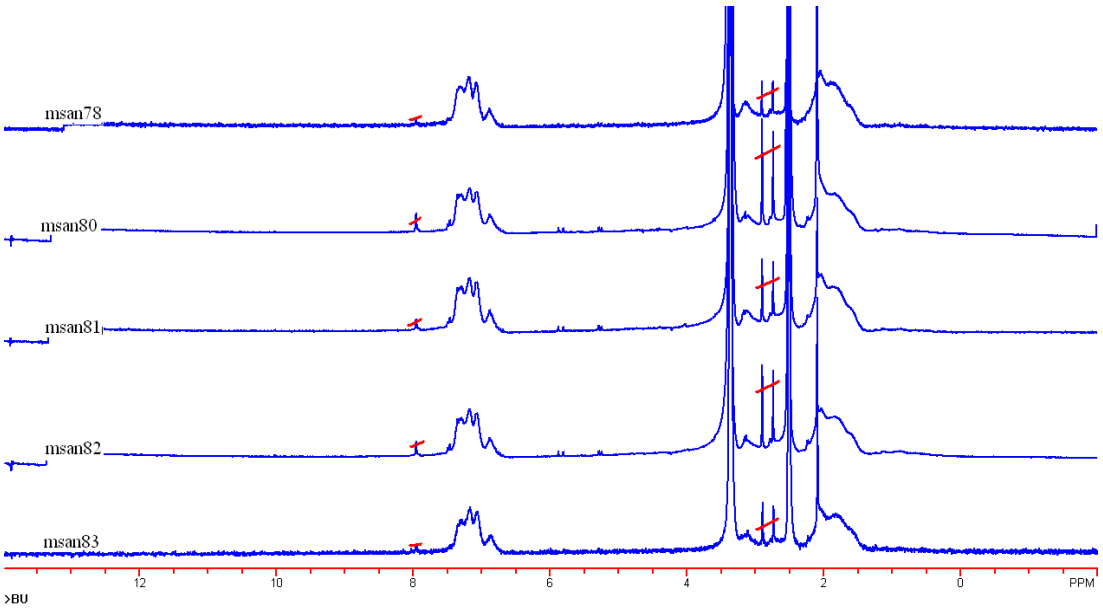

Figure 4.9 : ^{1}H-NMR spectra of MSAN78 and MSAN/NaMt80-81-82-83

Monomer ratio in copolymer chain were determined by 1H-NMR spectra. MSAN78 has a monomer ratio of 40% styrene units, 60% acrylonitrile units. MSAN/NaMt80 and MSAN/NaMt83 which include 0,5% and 2% NaMt respectively, have monomer ratio of 50% styrene, 50% acrylonitrile units. MSAN/NaMt81 and MSAN/NaMt82 which include 1% and 1,5% NaMt respectively, have monomer ratio of 44% styrene, 56% acrylonitrile units.

4.3 Rheologic, Mechanic, Thermal and Other Analysis

4.3.1 XRD analysis

X-ray diffraction analysis (XRD) was used to determine the interactions between NaMt layers and MSAN. The basic principle of XRD is the interference of waves reflected from different crystal planes [62]. The degree of dispersion of the clays can be assessed by X-ray diffraction. This can be achieved by monitoring the intensity and positioning of the d_{001} spacing, which reports the distance between stacks of parallel clay sheets [63]. Diffraction peak (d_{001}) of NaMt was observed at $2\theta=5^{o}$-9^{o} (Figure 4.10). However, no diffraction peak (d_{001}) was observed in composite samples (MSAN/NaMt80-81-82-83). One of the reasons might be the totally dispersing of NaMt layers. So, the diffraction peak might be shifted under $2\theta=2^{o}$. Moreover, NaMt might be totally covered with polymer preventing reflaction. This might be the other reason for absence of diffraction peak (d_{001}).

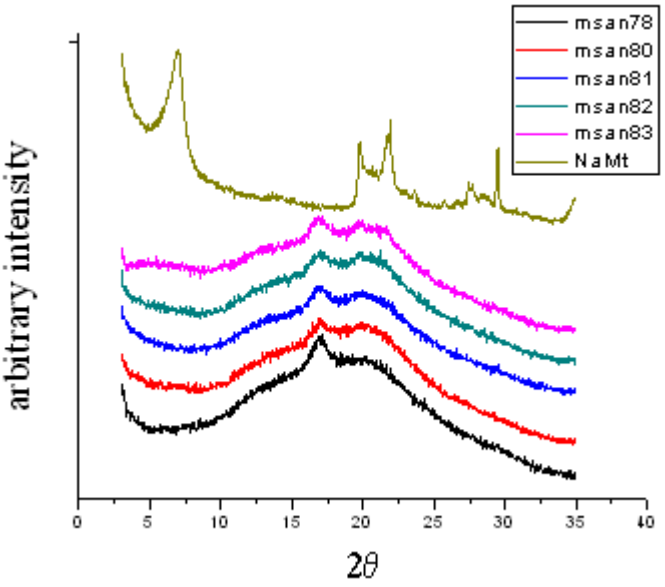

Figure 4.10 : XRD patterns of NaMt and nanocomposite including 2% NaMt (MSAN/NaMt83)

4.3.2 Rheology analysis

Temperature dependent rheologic properties of MSAN78 and MSAN/NaMt samples were determined by rheology analysis. 10% w/v solutions were prepared in DMF and measurements were performed at 20°C, 25°C and 30°C. Measurements were performed by increasing spindle speed from 100 rpm to 200 rpm (shear rate from 1400 s^{-1} to 2667 s^{-1}), and slowing back from 200 rpm to 100 rpm. Data was collected at every 5 rpm increment with a stabilizing time of 10 s before each measurement.

Rheology is the study of how a material deforms during and after a force is applied [64]. There are two types of fluids: Newtonian and Non-Newtonian (Figure 4.11). Newtonian Fluids are truly viscous "ideal liquids", which means as the shear rate changes the viscosity remains constant. Non-Newtonian Fluids are affected by shear and are divided into Power Law Fluids (Pseudoplastic, Dilatant or Bingham Plastic Model) and Time Dependent Fluids (Rheopectic or Thixotropic). In pseudoplastic behaviour, as shear stress increases, polymer chains disentangle and viscosity decreases. In dilatant behaviour, opposite of pseudoplastic, as shear stress increases, polymer chains entangle and the viscosity increases.

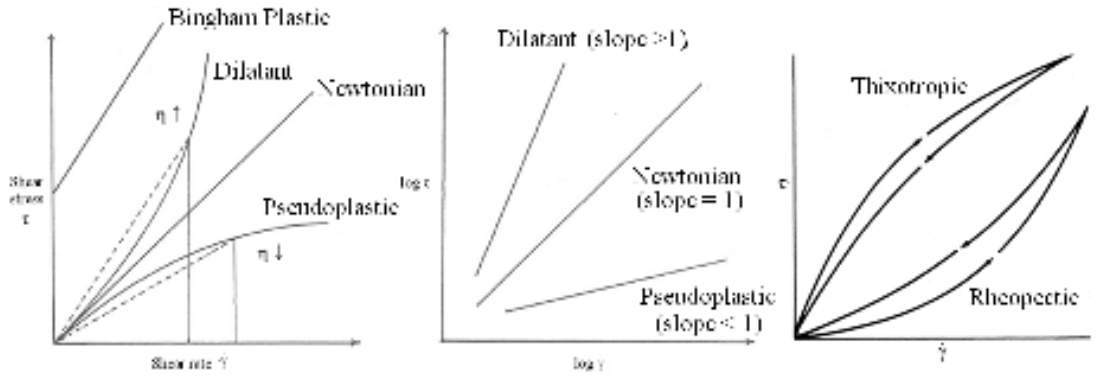

Figure 4.11 : Newtonian and Non-Newtonian flow curves

Bingham plastics have constant viscosity like Newtonian Fluids as shear rate changes but, they have an initial shear stress value different from "0" unlike Newtonian Fluids. Flow curves were analyzed using the Bingham model, where the Bingham yield stress τ is given by the relation (4.3)

$$\tau = \tau_B + \eta_{pl} \cdot \gamma \qquad \textbf{(4.3)}$$

Here τ_B is the extrapolated yield value (or critical sheare stress or threshold stress or initial resistance to flow) and η_{pl} is the plastic viscosity (or flow index). Once the curve of shear stress *vs*. shear rate was obtained for samples under the given experimental conditions, the value of the extrapolated shear stress was determined from the intersection of the extrapolated linear portion of the curve with the axis. The method of least squares was used to determine the values of this intersection. Plastic viscosity was derived from the slope of this linear section.

In rheopectic behaviour, viscosity increases as a function of time. In thixotropic behaviour as shear increases, the viscosity decreases.

Flow index is the indicator of flow character. It is determined by calculating slope of log shear stress- log shear rate plot [65]. If flow index is equal to 1, it is a Newtonian or Bingham plastic. If flow index is higher or smaller than 1, it is dilatant or pseudoplastic, respectively. Flow behaviour of MSAN78 and MSAN/NaMt samples were determined from shear stress versus shear rate plots.

MSAN78 and MSAN/NaMt samples displayed different time-independent behaviours. MSAN78 displayed Bingham plastic model. Log shear stress- log shear

rate plot of MSAN78 at 25°C and 30°C were given in Figure 4.12. Flow index values of MSAN78 are very close values to 1 at 25°C and 30°C (Table 4.3), So, it displayed Bingham plastic model at these temperatures.

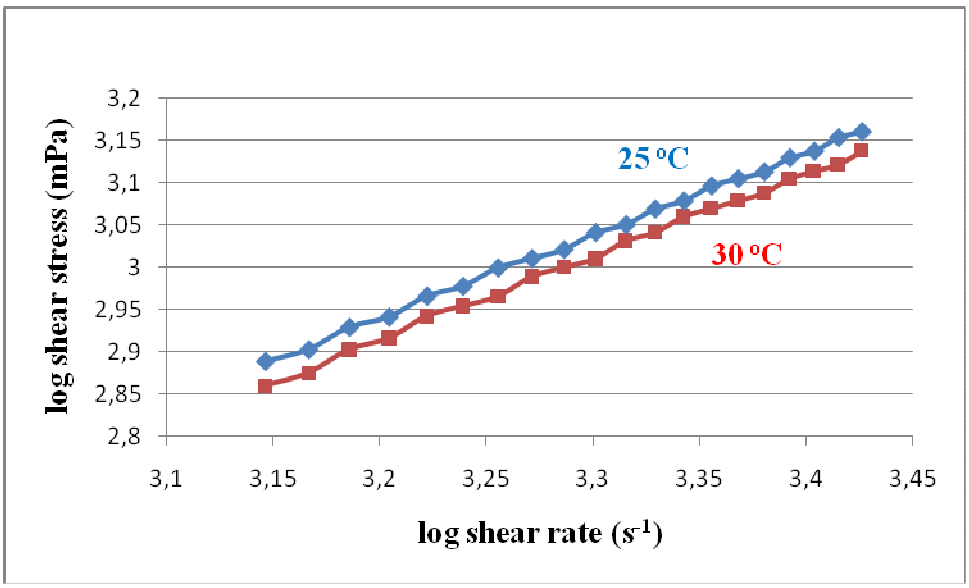

Figure 4.12 : Log shear stress- log shear rate plot of MSAN78 at 25°C and 30°C.

Table 4.3: Flow index and hysteresis area values of MSAN78- MSAN/NaMt80-81-82-83 at 20°C, 25°C and 30°C

Experiment	Flow index (Pa.s)			Hysteresis area (Pa.s^{-1})		
	20°C	25°C	30°C	20°C	25°C	30°C
MSAN78	0,93	0,98	0,99	7,53	19,05	31,59
MSAN/NaMt80	0,87	0,93	0,92	9,31	13,88	16,51
MSAN/NaMt81	0,76	0,78	0,80	19,17	20,76	22,57
MSAN/NaMt82	0,79	0,84	0,84	13,13	12,31	18,34
MSAN/NaMt83	0,84	0,87	0,88	19,11	28,86	38,21

Yield values (τ_B) of MSAN78 at 25°C and at 30°C are 63,116 and 18,367, respectively. A decrease in yield value was observed by the increase of temperature. Plastic viscosity values (η_{pl}) at 25°C and at 30°C are 0,6134 and 0,5069, respectively. A decrease in plastic viscosity value was observed by the increase of temperature as well. The reason of the decrease in yield value and plastic viscosity was thougth to be the increase of disentanglement by the increase of temperature.

Flow indexes of all of the nanocomposite samples are smaller than 1 (Table 4.3). So, it is decided them to displayed pseudoplastic behaviour while MSAN78 displayed Bingham plastic model. In the Figure 4.13, the flow index and NaMt percent were demonstrated. Flow indexes decreased by increasing amount of NaMt 0 % to 1% . Then an increase in flow index was observed 1% to 2%. In addition, a slight increase in flow indexes was observed by the increase of temperature 20°C to 30°C (Table 4.3, Figure 4.13). This results indicated a decrease in gelations with the first addition of NaMt. After that 1% NaMt addition gradual increased was observed. This may be caused by the increase in entanglement or flocculation by the increase of NaMt.

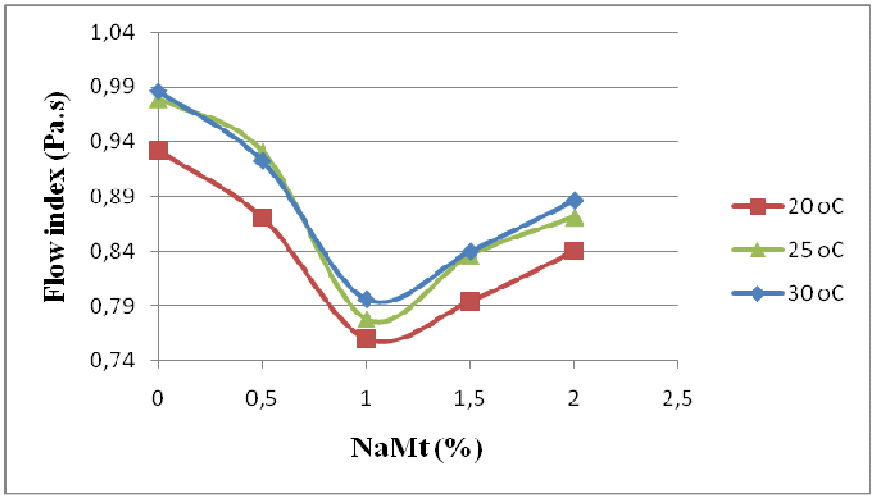

Figure 4.13 : Flow index versus NaMt percent plots at 20°C, 25°C and 30°C

The degree of thixotropic or rheopectic behaviour is measurement by the area of the hysteresis loop [66]. In other words, hysteresis area is the indicator of time-dependent behaviour. The area between upward and downward curve in shear stress-shear rate plot is called hysteresis area. Magnitude of hysteresis area is proportional with the time-dependent behaviour. Hysteresis area of samples were given in Table 4.3. MSAN78 and MSAN/NaMt samples displayed rheopectic behaviour. Shear stress-shear rate plot of MSAN/NaMt81 were given in Figure 4.14 demonstrating rheopectic behaviour of it as in all samples.

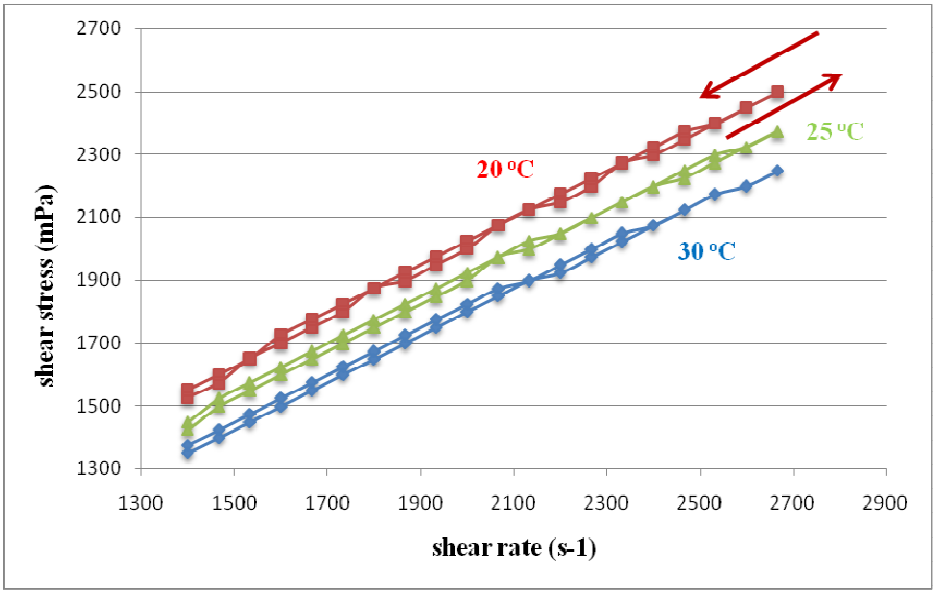

Figure 4.14 : Shear stress-shear rate plots of MSAN/NaMt81 at 20°C, 25°C and 30°C

Hysteresis area values tended to increase by the increase of temperature 20°C to 30°C. This indicates that an increase in rheopectic behaviour of samples were observed by increase of temperature (Table 4.3). However, increasing amount of NaMt caused a difference in the rheopectic behaviour (Figure 4.15a). This results indicated a gradual decrease in gelations with the first addition of NaMt. After that point increased was observed which reaches a maximum at 1% NaMt. Further addition of polymer resulted in an increase in the area of the hysteresis loop. This may be caused by the increase in entanglement by the increase after NaMt 1,5%.

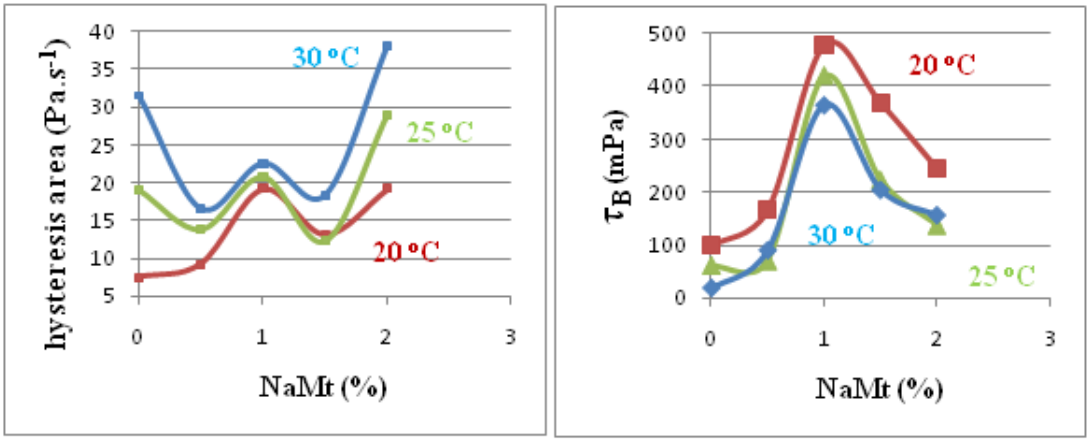

Figure 4.15 : **(a)** Hysteresis area versus NaMt percent plots at 20°C, 25°C and 30°C. **(b)** Yield value versus NaMt percent plots at 20°C, 25°C and 30°C

In the Figure 4.15b the yield value versus NaMt percent plots of MSAN78 and MSAN/NaMt samples were demonstrated. Figure 4.15b shows an increase in gelation till the NaMt 1% addition. However, furher addition of NaMt a clear decrease was observed. This curve agreed the curves in Figure 4.13 and Figure 4.15(a) since the maximum yield value were seen at around 1% NaMt addition in these figures. This point showed the maximum flocculation, after further addition, the system began deflocculation.

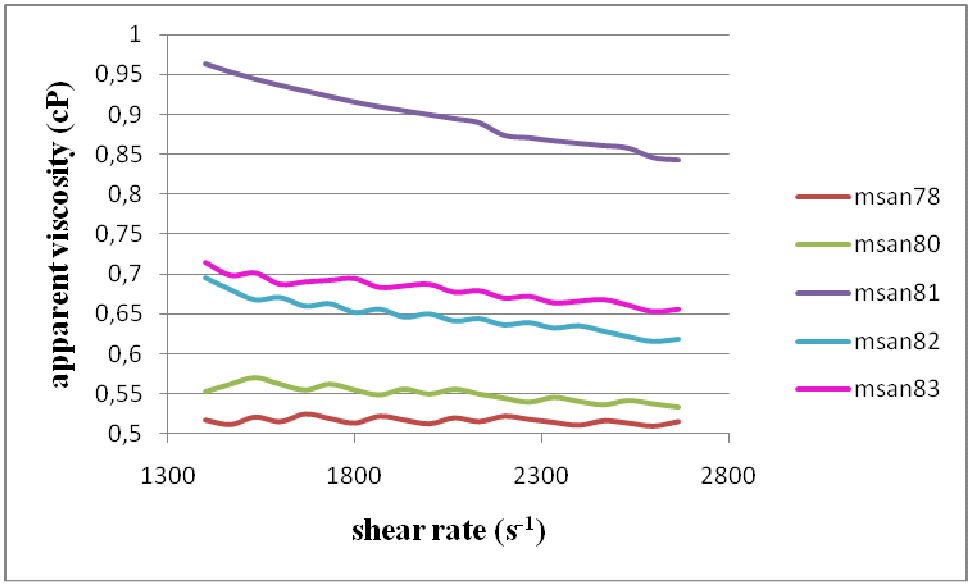

Figure 4.16 : Apparent viscosity versus shear rate plots of MSAN78 and MSAN/NaMt samples

The increase in the appearent viscosity with shear rate is due to the increase of number of NaMt particles in the dispersion (Figure 4.16. The NaMt has naturally a higher appearent viscosity, because NaMt have smaller particle size, a greater number of clay particles in dispersion and increased surface area of clay minerals. At the beginning, when η_{app} values were evaluated, it was thought that NaMt addition into the system would cause flocculation. It is possible that copolymer nonbonding interaction with oxygen atoms on the surface of NaMt minerals; thus, polymer molecules can attach on various places on clay surfaces. Polymer can hold on the clay surfaces and at the same time, some polymer molecules can attach to other clay surfaces and those already attached polymer molecules on the surface of other clay minerals may form bridging flocculation. For this reason, this new appearance in slurry could end up with flocculation.

4.3.3 DMA analysis

Mechanical resistance of molasses MSAN78 and MSAN/NaMt samples were determined by using DMA. In DMA, the sample is subjected to a periodically varying stress [67]. The respond of the sample to this treatment can provide information on the stiffness of the material and its ability to dissipate energy. Measurements were performed in 25^{o}C by determining strain versus stress plots. Young's modulus, strain and stress values are shown in Table 4.4.

Table 4.4: Young's modulus and breaking points of MSAN78 and MSAN/NaMt80-81-82-83 at 25^{o}C

Experiment	Young's Modulus (MPa)	Breaking Point	
		Stress (MPa)	Strain (%)
MSAN78	1670	4,764	0,1741
MSAN/NaMt80	2156	10,95	0,4164
MSAN/NaMt81	2343	8,389	0,3141
MSAN/NaMt82	2532	16,28	0,7933
MSAN/NaMt83	2784	14,61	0,4784

According to the Young's modulus values, elasticity of nanocomposite samples increase by the increase of NaMt amount that they include. When the breaking points are observed, it can be seen that the rupture of MSAN78 film occurs in the lowest stress and strain values. Young's modulus and breaking point values support the copolymer sample with no NaMt content (MSAN78) to have the lowest mechanical resistance. This proves the interaction between the copolymer and NaMt and there is an obvious enhancement in mechanical resistance by this interaction. The rupture occurs in different stress and strain values for nanocomposite samples including different NaMt amounts. According to the breaking point values, composite film with 1% NaMt (MSAN/NaMt81) has a less durability than composite film with 0,5% NaMt (MSAN/NaMt80). Likewise, nanocomposite film with 2% NaMt (MSAN/NaMt83) has a less durability than composite film with 1,5% NaMt (MSAN/NaMt82). Composite sample which has the most enhanced mechanical resistance is composite film with 1,5 % NaMt (MSAN/NaMt82).

The reason of the difference in mechanical strength between composite samples may be concerning with the dispersion or flocculation of NaMt.

MSAN78, composite film with 1% NaMt (MSAN/NaMt81) and composite film with 2% NaMt (MSAN/NaMt83) demonstrated the enhancement in mechanical resistance

provided with NaMt interaction. Strain versus stress plots of MSAN78 and composites prepared with 1% (MSAN/NaMt81) and 2% (MSAN/NaMt83) NaMt are demonstrated in Figure 4.17.

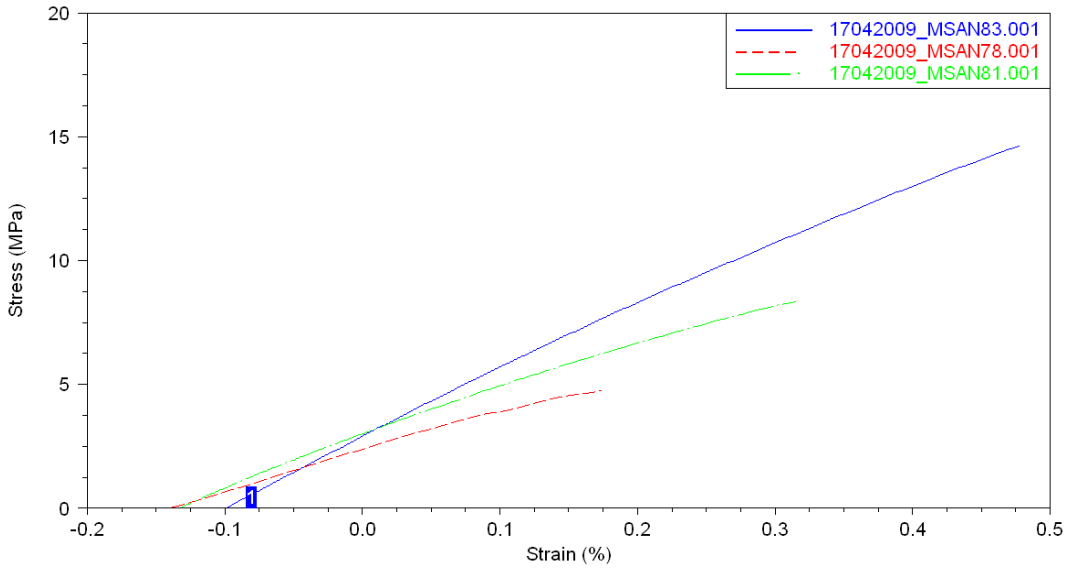

Figure 4.17 : Strain versus stress plots of MSAN78, MSAN/NaMt81 and MSAN/NaMt83 at 25°C

4.3.4 DSC analysis

Some physical properties of molasses, MSAN78 and MSAN/NaMt samples were determined by DSC. DSC is an analytical technique for detecting the changes in physical states of matter by measuring the energy necessary to establish a nearly zero temperature difference between a substance and an inert reference material, as the two specimens are subjected to identical temperature regimes in an environment heated or cooled at a controlled rate [68]. It is based on the thought that the thermal properties of a material are dependent upon changes in its structure and mobility. Measurements were performed as first heating, cooling and second heating under N_2 atmosphere. For MSAN and MSAN/NaMt samples, first heating was applied from -90°C to 150°C with a ramp rate of 20,0°C/min, then cooled to -90°C and second heating was applied from -90°C to 400°C. For molasses, first heating was applied from -90°C to 130°C with a ramp rate of 20,0°C/min, then cooled to -90°C and second heating was applied from -90°C to 250°C Glass transition temperature (Tg), melting point (Tm) and decomposition temperatures (Td) of molasses, copolymer and nanocomposite samples were determined (Table 4.5).

Table 4.5: Glass transition, melting and decomposition temperatures of molasses, MSAN78 and MSAN/NaMt80-81-82-83

	Tg_1 (^oC)	Tg_2 (^oC)	Tm (^oC)	Td (^oC)
Molasses	-68,55	-	129,39	*
MSAN78	-54,81	102,65	194,85	310,37
MSAN/NaMt80	-52,19	101,67	197,51	313,13
MSAN/NaMt81	-54,42	102,87	198,76	312,03
MSAN/NaMt82	-57,47	102,02	199,53	310,76
MSAN/NaMt83	-59,48	99,43	197,43	312,84

*Not heated until decomposition

MSAN78 and nanocomposites of it displayed two glass transitions. First of the Tg was thought to proceed from molasses content in copolymer. Sopade et al. studied on glass transition of molasses and determined different types of molasses have Tg between -75^{o}C to -35^{o}C [69]. So, the endothermic event at -68,55^{o}C was thought to be the glass transition of molasses. The increase of Tg_1 in copolymer and nanocomposites of it, may be an evidence of reaction between monosaccharides and copolymer chain. The decrease in Tg_1 by the increase of NaMt amount, may also be the effect of arrengement of NaMt layers. Second glass transition of copolymer and nanocomposites of it occurs at about 102^{o}C (Table 4.5). Big differences in Tg_2 values were not observed. Ravi et al. determined the melting point of SAN at about 220^{o}C [70]. So, the endothermic event at about 200^{o}C was thought to be the melting of copolymer. There is generally an upward trend in melting points (Tm) by the increase of NaMt amount. This may be the evidence of enhancement in thermal stability provided by interactions between NaMt and copolymer. SAN is known to begin to decompose at about 260^{o}C [70]. As seen in the thermograms of MSAN78 and MSAN/NaMt81, (Figure 4.18), exothermic event which have the maximum temperature at about 310^{o}C is thought as the decomposition of copolymer. It can be said there is an enhancement in thermal stability by the increase of NaMt amount.

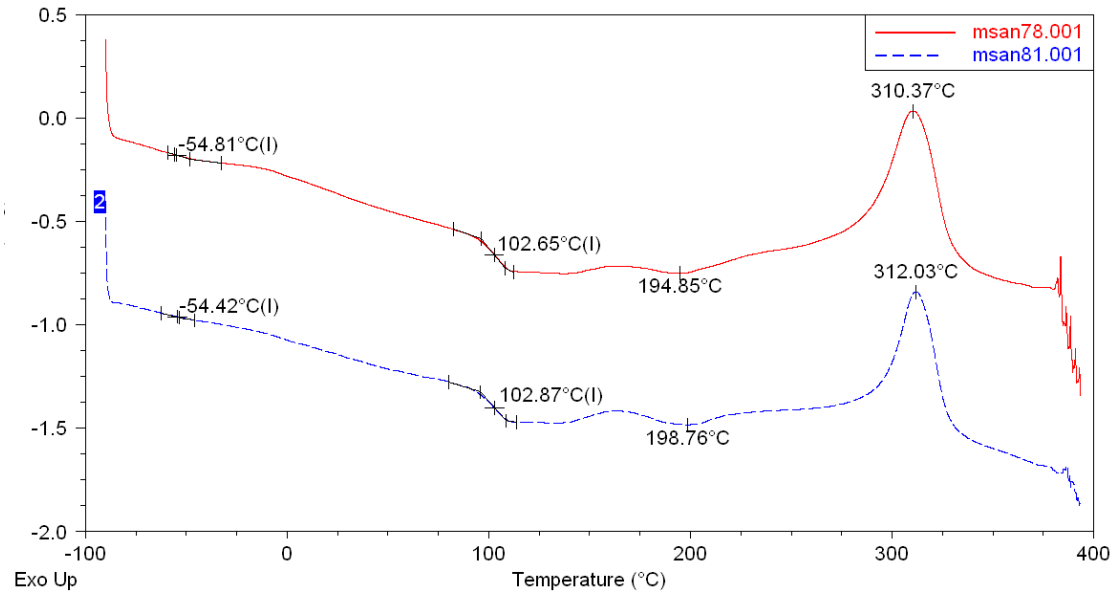

Figure 4.18 : DSC thermograms of MSAN78 and NaMt-nanocomposite of it including 1% NaMt (MSAN/NaMt81)

4.3.5 TGA analysis

Thermal decomposition of MSAN78 and MSAN/NaMt samples were determined by using TGA. TGA is an instrumental method to heat a sample in a small pan by a programmed temperature change when flushing with an inert gas and at the same time continuously weighing the pan [71]. Measurements were carried out under N_2 atmosphere from 20°C to 600°C with a heating rate of 20°C/min. Signal maximum temperatures and percentage of residues were given in Table 4.6.

Table 4.6: Residue at 480°C and signal max values of MSAN78 and MSAN/NaMt samples

Experiment	Signal max(°C)	Residue at 480 °C (%)
MSAN78	427,73	25,10
MSAN/NaMt80	431,52	16,66
MSAN/NaMt81	430,86	17,67
MSAN/NaMt82	427,24	22,23
MSAN/NaMt83	432,94	19,55

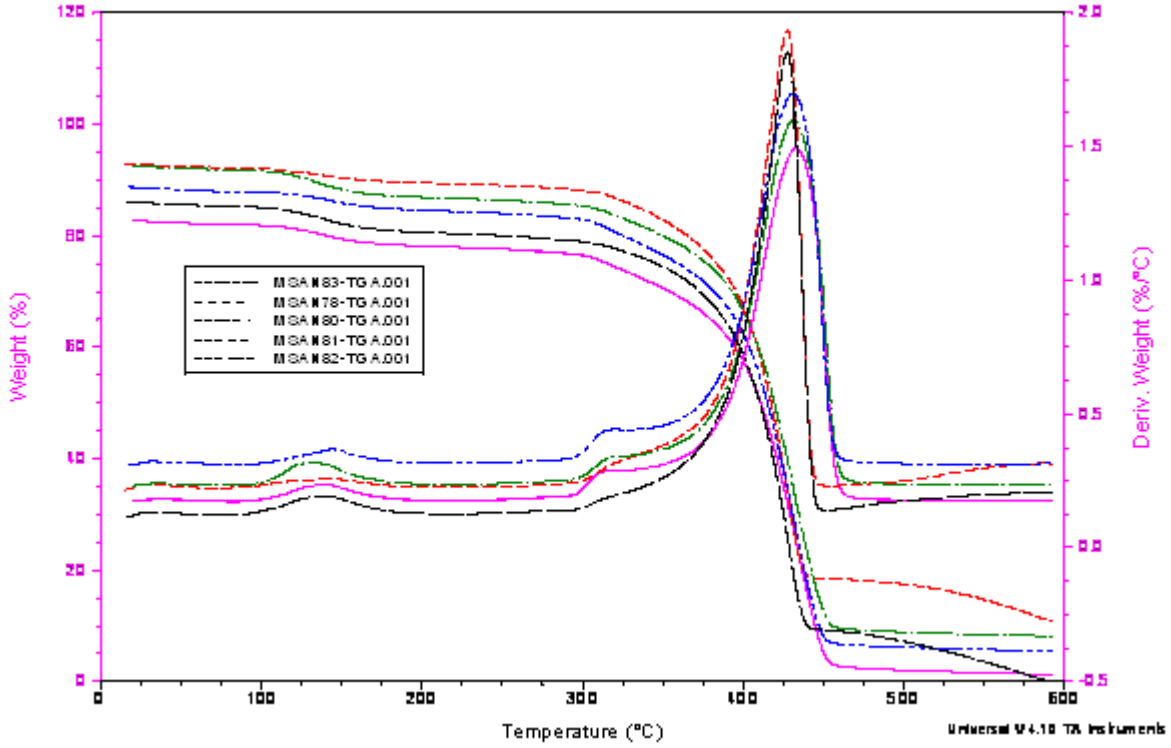

Figure 4.19 : TGA thermograms of MSAN78 and (MSAN/NaMt80, 81, 82,83)

As evident from the Figure 4.19, copolymer decomposition in the nanocomposites are found to moved to higher temperature, indicating the enhancement of thermal stability of composites. This enhancement of thermal stability can be regarded as an additional evidence of the interactions between copolymer and NaMt. It is also noticeable that the percentage of the residue lowered in NaMt-nanocomposite samples when compared with copolymer. Temperatures which 40%, 50% and 60% residues remained were given in Table 4.7. Temperatures increased in nanocomposites when compared with copolymer (MSAN78). This indicates that decompositions of composites are higher than that of copolymer. This is also an evidence of the interactions between copolymer and NaMt. MSAN/NaMt83 was determined as the most thermally stable nanocomposite sample with 2% NaMt amount. There is a slight decrease in temperatures at the residue percent remained, in MSAN/NaMt80, MSAN/NaMt81 and MSAN/NaMt82. The reason of this may be the arrangement of NaMt layers.

Table 4.7: Temperatures at 40%, 50% and 60% residue remained in MSAN78 and nanocomposites of it (MSAN/NaMt80-81-82-83)

Experiment	Temp. at 40% residue (^oC)	Temp. at 50% residue (^oC)	Temp. at 60% residue (^oC)
MSAN78	428,17	422,25	415,21
MSAN/NaMt80	432,28	425,50	417,32
MSAN/NaMt81	431,71	424,48	416,38
MSAN/NaMt82	427,39	421,46	414,01
MSAN/NaMt83	434,39	427,03	418,64

4.3.6 Water sorption

Water sorption tests were performed to determine water absorption of MSAN78 and MSAN/NaMt samples. Water sorption is performed by using discs in particular dimensions [72]. Water sorption is determined by calculation of ratio of weigth change and surface area of discs (4.4).

$$\text{Water sorption } (mg/cm^2) = \frac{w\text{-}W}{S} \qquad \textbf{(4.4)}$$

Where; w is weight after immersion in mg, W is conditioned weight in mg and S is surface area of the disc in cm^2.

Discs of MSAN78 and MSAN/NaMt samples were prepared in the dimensions of 40 ± 1 mm in diameter x 2 mm. Discs were dried at 130^oC and removed to a desiccator at room temperature for 1h before weighed. All of the discs were weighed. Then, discs were immersed into distilled water at 37 ± 1^oC for 24 h. After 24 h, they were removed from water, wiped with a clean dry towel removing visible moisture, waved in the air for 15 s and weighed after 1 min after their removal from the water. After data was collected, water sorption was calculated. The results were given in Figure 4.20.

As seen in Figure 4.20, water sorption decreased by increasing amount of NaMt. MSAN78 has the most water sorption. Nanocomposite samples with increasing amount of NaMt have less water sorption and it stabilized at 1,5% and 2% NaMt percentage. It is obvious that NaMt provided a good water resistance to MSAN.

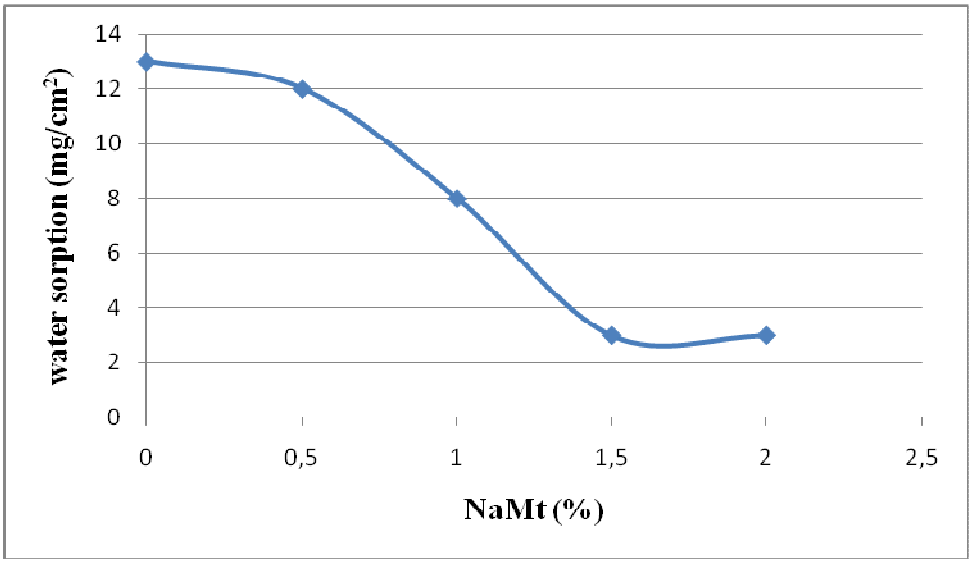

Figure 4.20 : Water sorption of MSAN78 and nanocomposites of it with increasing NaMt percentage

5. CONCLUSION AND RECOMMENDATIONS

Synthesis and characterization of MSAN and MSAN/NaMt samples, can be summarized as follows;

- MSAN was synthesized by using Ce(IV)/HNO_3 redox pair as initiator with emulsion polymerization.
- Optimum reaction conditions were determined as 12 g/L molasses, 0,95 mole/L acrylonitrile, 0,33 mole/L styrene, 47,4 mmole/L Ce(IV), 28,7 mmole/L HNO_3.
- MSAN78 was obtained with optimum reaction conditions with a yield of 82%.
- Monomer ratio of obtained copolymer was 40% styrene units and 60 % acrylonitrile units in copolymer chain.
- MSAN/NaMt samples were synthesized by *in situ* polimerization in the amounts of 0,5%, 1%, 1,5% and 2% NaMt in the same reaction conditions with MSAN78.
- MSAN/NaMt samples were obtained with a yield of 58%.
- Monomer ratio of obtained copolymer was 50% styrene units and 50 % acrylonitrile units in copolymer chain for 0,5% and 2% NaMt including nanocomposites and 44% styrene units and 56% acrylonitrile units for 1% and 1,5% NaMt including nanocomposites, respectively.
- FT-IR and ^{1}H-NMR analysis demonstrated the synthesis of MSAN and MSAN/NaMt samples were achieved successfully.
- Thermal analysis (DSC and TGA) demontrated that MSAN/NaMt samples acquired superior thermal stability than MSAN78.
- DMA analysis demonstrated that mechanical resistance of MSAN/NaMt samples increased by the increasing amount NaMt.

- Water resistance of MSAN/NaMt samples demonstrated an obvious enhancement by increasing amount of NaMt.
- TEM and SEM analysis should be performed to determine and commentate the properties of nanocomposites better.

REFERENCES

[1] **Chanda, M. and Roy, S. K.**, 2009, Industrial Polymers, in *Industrial Polymers, Specialty Polymers, and Their Applications*. CRC Press. p. 39.

[2] **Garlinghouse, S. E.** High energy feeds (grains, liquid supplements,by-products). <http://shady-acres.com/susan/7.html>, accessed at 15.09.2008.

[3] <http://running_on_alcohol.tripod.com/id21.html>, accessed at 03.08.2008.

[4] **Kochergin, V. and Kearney, M.** Chromatographic Seperator Optimization. 1995.<http://www.arifractal.com/assbt%201995%20smb%20optimization.pdf>, accessed at 16.08.2008

[5]<http://www.agmrc.org/commodities__products/grains__oilseeds/sugar_beet_profile.cf>, accessed at 27.10.2008

[6] <http://www.turkseker.gov.tr/KurumIstatistikleri.aspx>, accessed at 12.12.2008.

[7] **Avcı, A.**, 2004, Bazı Thermoanaerobacter suşlarının etanol üretim oranlarının karşılaştırılması, *M.Sc. Thesis*, Ankara University.

[8] <http://www.premiermolasses.ie/standard.htm>, accessed at 03.01.2009.

[9] <http://www.premiermolasses.ie/uses.htm>, accessed at 03.01.2009.

[10] **Jumadurdiyev, A., Ozkul, M. H., Saglam, A. R. and Parlak, N.**, 2005, The utilization of beet molasses as a retarding and water-reducing admixture for concrete. *Cement and Concrete Research*, **35**(5): p. 874-882.

[11] **Lotfy, W. A.**, 2007, The utilization of beet molasses as a novel carbon source for cephalosporin C production by Acremonium chrysogenum: Optimization of process parameters through statistical experimental designs. *Bioresource Technology*. **98**(18): p. 3491-3498.

[12] **Yang, B. Y. and Montgomery, R.**, 2007, Alkaline degradation of invert sugar from molasses. *Bioresource Technology*. **98**(16): p. 3084-3089.

[13] **Nagarajan, S. and Srinivasan, K. S. V.**, 1998, Efficiency of ceric ione for oxidation and polymerization - A review. *Journal of Macromolecular Science-Reviews in Macromolecular Chemistry and Physics*. **C38**(1): p. 54.

[14] **Nagarajan, S. and Srinivasan, K. S. V.**, 1998, Efficiency of ceric ione for oxidation and polymerization - A review. *Journal of Macromolecular Science-Reviews in Macromolecular Chemistry and Physics*. **C38**(1): p. 54-55.

[15] **Trahanovsky, W. S. and Young, L. B.**, 1966, Controlled oxidation of organic compounds with Cerium(IV). II. The oxidation of toluenes. *Journal of Organic Chemistry*. **31**(6): p. 2033.

[16] **Duke, F. R.**, 1947, *Journal of The American Chemical Society*. **69**: p. 2885.

[17] **Mino, G. and Kaizerman, S.**, 1958, A new method for the preparation of graft copolymers. Polymerization initiated by ceric ion redox systems. *Journal of Polymer Science*. **31**: p. 242.

[18] **Yağcı, Y., Reetz, I. and Mishra, M. K.**, 2009, Chemical Initiation by metals or metal-containing compounds, in *Handbook of Vinyl Polymers*

Radical Polymerization, Process, and Technology, Y. Yağcı and M. K. Mishra, Editors, CRC Press. p. 59-60.

[19] **Pramanick, D. and Sarkar, S. K.**, 1976, Mode of initiation in ceric salt initiated aqueous polymerization of methylmethacrylate. *Colloid and Polymer Science*. **254**(11): p. 989.

[20] **Akar, A., Galioglu, O., Gocmen, A. and Sarac, A. S.**, 1990, Copolymer of Ketonic Resin-Polyacrylonitrile. *Journal of Applied Polymer Science*. **39**(8): p. 1657-1663.

[21] **Galioglu, O., Soydan, A. B., Akar, A. and Sarac, A. S.**, 1994, Block and graft copolymer synthesis via ceric salt. *Angewandte Makromolekulare Chemie*. **214**: p. 19-28.

[22] **Öz, N. and Akar, A.**, 2006, Redox initiation system of ceric salt and dihydroxy poly(dimethylsiloxane)s. *Journal of Applied Polymer Science*. **102**: p. 2112.

[23] **Bajpai, U.D.N.**, 1996, Guar (Graft copolymerization), in *Polymeric Materials Encyclopedia*, J. C. Solomone, Editor, CRC Press Inc: Florida. p. 188.

[24] Kagaku N. Co. Ltd., Japan, Jpn. Patent 55165909, 1980; CA: 94(22), 17706n, 1994.

[25] **Sharma, B. R., Kumar, V. and Soni, P. L.**, 2002, Ceric ammonium nitrate-initiated graft copolymerization of acrylamide onto Cassia tora gum. *Journal of Applied Polymer Science*. **86**(13): p. 3250-3255.

[26] **Choi, K. Y., Kwag, B.G., Park, S.Y. and Cheong, C. H.**, 2009, Technical Processes for Industrial Production, in *Handbook of Vinyl Polymers Radical Polymerization, Process, and Technology*, M. K. Mishra and Y. Yagci, Editors, CRC Press. p. 389-390.

[27] **Choi, K. Y., Kwag, B.G., Park, S.Y. and Cheong, C. H.**, 2009, Technical Processes for Industrial Production, in *Handbook of Vinyl Polymers Radical Polymerization, Process, and Technology*, M. K. Mishra and Y. Yagci, Editors, CRC Press. p. 387-389.

[28] **Tripathi, S. and Srivastava, A. K.**, 2007, Kinetics and mechanism of copolymerization of styrene with acrylonitrile using triphenylbismuthonium 1,2,3,4-tetraphenylcyclopentadienylide as the radical initiator. *Polymer-Plastics Technology and Engineering*. **46**(3): p. 213-218.

[29] **Choi, K. Y., Kwag, B.G., Park, S.Y. and Cheong, C. H.**, 2009, Technical Processes for Industrial Production, in *Handbook of Vinyl Polymers Radical Polymerization, Process, and Technology*, M. K. Mishra and Y. Yagci, Editors., CRC Press. p. 390.

[30] **Mino, G.**, 1956, Copolymerization of styrene and acrylonitrile in aqueous dispersion. *Journal of Polymer Science*. **22**(102): p. 369-383.

[31] **Medizabal, E., Rodriguez-Ruvalcaba, R., Rabelero, V., Puig, J. E., Velazquez, R. and Castano, V.**, 1995, A Comparison of emulsion and microemulsion copolymerization of styrene and acrylonitrile, *International Journal of Polymeric Materials*. **30**(3-4): p. 167-179.

[32] **Vanderhoff, J. W., Dimonie, V., El-Aasser, M. S. and Klein, A.**, 1993, Emulsion copolymerization of azeotropic styrene-acrylonitrile monomer mixture in polystyrene seed latexes. *Die Makromolekulare Chemie*. **10**(S19851): p. 391-402.

[33] **Lin, C.C., Ku, H.C. and Chiu, W.Y.**, 1981, Simulation model for the emulsion copolymerization of acrylonitrile and styrene in azeotropic composition. *Journal of Applied Polymer Science*. **26**(4): p. 1327 - 1342.

[34] **Choi, K. Y., Kwag, B.G., Park, S.Y. and Cheong, C. H.**, 2009, Technical Processes for Industrial Production, in *Handbook of Vinyl Polymers Radical Polymerization, Process, and Technology*, M. K. Mishra and Y. Yagci, Editors, CRC Press. p. 390-391.

[35] **Kido, K., Wakamori, H., Asai, G. and Kushida, K.**, 1978, *Jpn. Kokai Tokkyo Koho*. **JP 78,126,094**.

[36] **Kato, S. and Momoka, M.**, *Jpn. Kokai Tokkyo Koho*. **JP 7,882,892** (89,180616z).

[37] **Choi, K. Y., Kwag, B.G., Park, S.Y. and Cheong, C. H.**, 2009, Technical Processes for Industrial Production, in *Handbook of Vinyl Polymers Radical Polymerization, Process, and Technology*, M. K. Mishra and Y. Yagci, Editors., CRC Press. p. 391.

[38] **Arsac, A., Zerroukhi, A., Ainser, A. and Carrot, C.**, 2000, Rheological characterization of styrene acrylonitrile copolymers. *Journal of Applied Polymer Science*. **77**(6): p. 1316-1321.

[39] **Al-Harthi, M., Sardashti, A., Soares, J. B. P. and Simon, L. C.**, 2007, Atom transfer radical polymerization (ATRP) of styrene and acrylonitrile with monofunctional and bifunctional initiators. *Polymer*. **48**(7): p. 1954-1961.

[40] **Carrado, K. A.**, 2003, Polymer–Clay Nanocomposites, in *Advanced Polymeric Materials-Structure Property Relationships*, G. O. Shonaike and S. G. Advani, Editors., CRC Press. p. 1-3.

[41] **Carrado, K.A.**, 2003, Polymer–Clay Nanocomposites, in *Advanced Polymeric Materials-Structure Property Relationships*, G. O. Shonaike and S. G. Advani, Editors, CRC Press. p. 4-12.

[42] **Wang, H. W., Chang, K. C. and Chu, H. C.**, 2005, Effect of clay on the properties of poly(styrene-co-acrylonitrile)-clay nanocomposites. *Polymer International*. **54**(1): p. 114-119.

[43] **Stretz, H. A. and Paul, D. R.**, 2006, Properties and morphology of nanocomposites based on styrenic polymers. Part I: Styrene-acrylonitrile copolymers. *Polymer*. **47**(24): p. 8123-8136.

[44] **Jang, B. N. and Wilkie, C. A.**, 2005, The effects of clay on the thermal degradation behavior of poly(styrene-co-acrylonitirile). *Polymer*. **46**(23): p. 9702-9713.

[45] **Khalil, H., Mahajan, D. and Rafailovich, M.**, 2005, Complex formation of montmorillonite clay with polymers. Part 2: The use of montmorillonite clay-vinyl monomer complex as a comonomer in the copolymerization reaction of styrene-acrylonitrile monomers. *Polymer International*. **54**(2): p. 428-436.

[46] **Noh, M. H. and Lee, D. C.**, 1999, Comparison of characteristics of SAN-MMT nanocomposites prepared by emulsion and solution polymerization. *Journal of Applied Polymer Science*. **74**(12): p. 2811-2819.

[47] **Ünlü, Cüneyt H., Günister, Ebru and Atıcı, Oya**, 2008, Synthesis and characterization of NaMt biocomposites with corn cob xylan in aqueous media. *Carbohydrate Polymers*.

[48] **Atici, O. G., Akar, A., Ayar, Y. and Mecit, O.**, 1999, Synthesis of block copolymers via redox polymerization. *Journal of Applied Polymer Science*. **71**(9): p. 1388.

[49] **Nagarajan, S. and Srinivasan, K. S. V.**, 1998, Efficiency of ceric ione for oxidation and polymerization - A review. *Journal of Macromolecular Science-Reviews in Macromolecular Chemistry and Physics*. **C38**(1): p. 55-56.

[50] **Czappa, D. J.**, 1974, The role of acid in the cerium (IV) oxidation of carbohydrates, *PhD Thesis*, The Institute of Paper Chemistry, Lawrence University.

[51] **Kacurakova, M., Capek, P., Sasinkova, V., Wellner, N. and Ebringerova, A.**, 2000, FT-IR study of plant cell wall model compounds: pectic polysaccharides and hemicelluloses. *Carbohydrate Polymers*. **43**(2): p. 195-203.

[52] **Silva, A. L. A., Takase, I., Pereira, R. P. and Rocco, A. M.**, 2008, Poly(styrene-co-acrylonitrile) based proton conductive membranes. *European Polymer Journal*. **44**(5): p. 1462-1474.

[53] **Clark, S., Barnett, N. W., Adams, M., Cook, I. B., Dyson, G. A. and Johnston, G.**, 2006, Monitoring a commercial fermentation with proton nuclear magnetic resonance spectroscopy with the aid of chemometrics, 338-345, 10.1016/j.aca.2005.11.033, ISI:000236570900042

[54] **Drake, E. N. and Brown, C. E.**, 1977, Conformational analysis of sugars by 1H NMR spectroscopy and polarimetry. *Journal of Chemistry*. **54**(124): p. 7.

[55]<http://hmdb.ca/labm/servlet/labm.mlims.showFile?tbl=tbl_hnmrv&id=1219789 35435965822>, accessed at 05.03.2009.

[56] **Boduroğlu, S.**, 2006, New Supramolecular Approach for Sugar Analysis, *PhD Thesis*, The Graduate Faculty of the University of Akron, University of Akron.

[57] **Jun, J. B., Uhm, S. Y. and Suh, K. D.**, 2003, Preparation and electrorheological characterization of suspensions of monodisperse micron-sized styrene-acrylonitrile copolymer particles. *Macromolecular Chemistry and Physics*. **204**(3): p. 451-459.

[58] **Simons, W.W. and Zanger, M.**, 1973, The Sadtler Guide to The NMR Spectra of Polymers. Philadelphia: Sadtler research laboratories, Inc. Sabsidiary of block engineering, Inc. 42.

[59] **Simons, W.W. and Zanger, M.**, 1973, The Sadtler Guide to The NMR Spectra of Polymers. Philadelphia: Sadtler research laboratories, Inc. Sabsidiary of block engineering, Inc. 52.

[60]<http://www.muhlenberg.edu/depts/chemistry/chem201woh/1Hdmf.html> accessed at 16.03.2009.

[61] **Gal, Y. S., Jin, S. H. and Kim, S. H.**, 2006, Synthesis and characterization of ionic polyacetylene derivative with azobenzene moieties. *Journal of Industrial and Engineering Chemistry*. **12**(2): p. 235-240.

[62] **Vahaplar, Kadir**, 2007, Structural and magnetic properties of Si(100)/Ta/Co multilayers for spintronics applications, *M.Sc Thsis*, Graduate School of Engineering and Sciences, İzmir Institute of Technology.

[63] **Greenfield, D. and Clegg, F.C.**, 2004, Enhancement of barrier properties in organic coatings using nanocomposites. *The Journal of Corrosion Science and Engineering*. **8**(8).
[64] <http://www.kitpackers.com/PDFs/TT-UnderstandingRheology.pdf>, accessed at 05.02.2009.
[65] **Djordjevic, D.**, 1992, Coextrusion. 15.
[66] **Mezger, Thomas G.**, 2006, The rheology handbook: for users of rotational and oscillatory rheometers. 2 ed: Vincentz Network GmbH & Co KG. 299.
[67] **Brown, Michael E.**, 2001, Introduction to thermal analysis: techniques and applications. 2, illustrated ed: Springer. 264.
[68] **Yang, H.L.** , 2006, Controlling the stereoregularıty of polyacrylonitrile and its determination using small molecule host inclusion compounds, *M.Sc. Thesis*, the Graduate Facultv of North Carolina State University, North Carolina State University, No of Pages.
[69] **Sopade, P. A., Lee, S. B., White, E. T. and Halley, P. J.**, 2007, Glass transition phenomena in molasses. *Lwt-Food Science and Technology*. **40**(6): p. 1117-1122.
[70] **Ravi, P. and Divakar, S.**, 2000, beta-cyclodextrin mediated synthesis of sterically controlled styrene-acrylonitrile copolymer. *Journal of Inclusion Phenomena and Macrocyclic Chemistry*. **38**(1-4): p. 323-336.
[71] **Wiehe, Irwin A.**, 2008, Process Chemistry of Petroleum Macromolecules: CRC Press. 456.
[72] **Snell, Foster Dee and Ettre, Leslie S.**, 1971, Water Sorption, in *Encyclopedia of Industrial Chemical Analysis* Interscience Publishers, 11, 302-306

CURRICULUM VITA

Name and Surname **:** Nurhan KADAK

Place and date of birth **:** ISTANBUL/ 07.02.1983

Permanent Address **:** Cumhuriyet mah Aşık Veysel cad. Mine sok. Kent Apt.No:2 D:7 Küçükçekmece/İSTANBUL

University attended **:** Chemistry Department/Istanbul Technical University

Publications:

Atıcı O., İşçi S., Kadak N., Synthesis and Characterization of Poly(acrylonitrile-*g*-methyl cellulose)/Organoclay Nanocomposites. *National Clay Symposium,* October 2007, Kütahya, Turkey.